



High agricultural water consumption led to the continued shrinkage of the Aral Sea during 1992–2015



Yanan Su ^a, Xin Li ^{b,c,d,*}, Min Feng ^{b,c,d}, Yanyun Nian ^a, Lingxin Huang ^a, Tingting Xie ^a, Kun Zhang ^b, Feng Chen ^{f,g}, Wei Huang ^a, Jianhui Chen ^a, Fahu Chen ^{a,e}

^a Key Laboratory of Western China's Environmental Systems (Ministry of Education), College of Earth and Environmental Sciences, Lanzhou University, Lanzhou 730000, China

^b National Tibetan Plateau Data Center, Key Laboratory of Tibetan Environmental Changes and Land Surface Processes, Institute of Tibetan Plateau Research, Chinese Academy of Sciences, Beijing 100101, China

^c CAS Center for Excellence in Tibetan Plateau Earth Sciences, Chinese Academy of Sciences, Beijing 100101, China

^d University of Chinese Academy Sciences, Beijing 100049, China

^e Key Laboratory of Alpine Ecology, CAS Center for Excellence in Tibetan Plateau Earth Sciences and Institute of Tibetan Plateau Research, Chinese Academy of Sciences (CAS), Beijing 100101, China

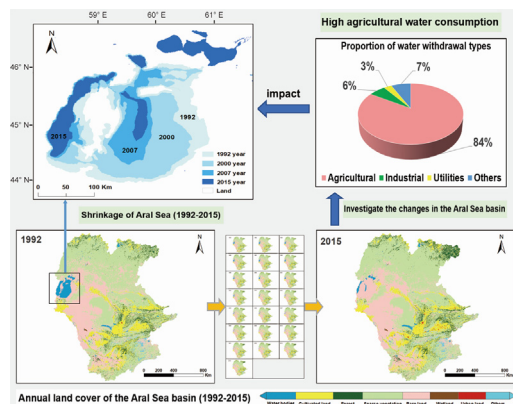
^f Institute of International Rivers and Eco-Security, Yunnan University, Kunming, China

^g Key Laboratory of Tree-ring Physical and Chemical Research of China Meteorological Administration/Xinjiang Laboratory of Tree-ring Ecology, Institute of Desert Meteorology, China Meteorological Administration, Urumqi, China

HIGHLIGHTS

- About 50.38% of the Aral Sea water area in 1992 turned into bare land by 2015.
- Climate change had a positive effect on the water supply of Aral Sea.
- No large-scale increase of farmland in the Aral Sea basin since the 1990s.
- High water consumption of agriculture led to the continued shrinkage of the Aral Sea.

GRAPHICAL ABSTRACT



ARTICLE INFO

Article history:

Received 17 November 2020

Received in revised form 13 February 2021

Accepted 14 February 2021

Available online 20 February 2021

Editor: Kuishuang Feng

Keywords:

Land cover

Aral Sea

Surface water

Agriculture

Human activities

ABSTRACT

The shrinkage of the Aral Sea started in the 1960s, and it has been continued for decades due to arguably both human and natural causes. However, the change of the Aral Sea in the post-Soviet era and its correlations with other changes in the extent of the basin have yet to be fully investigated. Here, we studied the land cover dynamics of the entire Aral Sea basin during 1992–2015 from the perspective of the surrounding environment, in order to investigate the causes of the Aral Sea further shrinkage in recent years. We used the annual Climate Change Initiative (CCI) land cover dataset to provide a spatiotemporally consistent delineation of land cover throughout the period. We found that: (1) In recent years, the Aral Sea continued shrinkage, approximately 50.38% of its water area in 1992 had dried out and turned into bare land by 2015. (2) The cultivated land area remained stable with a slight increase during the period, suggesting that no large-scale abandonment or expansion of farming extent occurred in the post-Soviet era. (3) Among other land types, urban areas are small and slightly expand at a rate of $0.024 \times 10^4 \text{ km}^2/\text{year}$, suggesting urbanization, and likely contribute to more water consumption. Our investigation also found that climate warming increased the upstream runoff, which has a positive effect on the water supply of the Aral Sea. The impact of human activity on the Aral Sea is more pronounced than climate

* Corresponding author.

E-mail address: xinli@itpcas.ac.cn (X. Li).

change. Therefore, the continued shrinkage of the Aral Sea was likely due to high water consumption of agriculture continues to exert the influence that existed in the 1960s. Other factors, such as urbanization have exacerbated this effect. The study examined the continued shrinkage of the Aral Sea in post-Soviet era, to provide an insight into the driving factors of the complex and still controversial Aral Sea crisis.

© 2021 Elsevier B.V. All rights reserved.

1. Introduction

Located in the arid region of central Asia, the Aral Sea was the largest terminal water body until the second half of the 20th century (Micklin, 2010). The Aral Sea has shrunk significantly since the 1960s due to extensive farmland irrigation, and most of the lake area has turned into bare land (Micklin, 1992; Shi et al., 2014; Wurtsbaugh et al., 2017). The reduction in lake area leads to rising lake surface temperatures and frequent sandstorms, which pose a serious threat to the surrounding ecological environment (Small et al., 2001; Indoitu et al., 2015; Jin et al., 2017).

The shrinkage of the Aral Sea is a result of the complex influences from both human and natural dimensions on the extent of not only the Aral Sea but also the entire basin (Lioubimtseva, 2014). As the largest inland river basin in the arid region of central Asia, the Aral Sea basin is a typical area for transnational watershed research (Conrad et al., 2016; Löw et al., 2018). The population and economic activities in the basin are closely related to the hydrometeorological conditions of the Pamir and Tianshan mountains (Lioubimtseva, 2015). Unbalanced water distribution is a major challenge facing the region (Bekchanov et al., 2016). Especially after the dissolution of the Soviet Union in 1991, the political and economic changes in central Asia intensified the water conflicts among countries, making the Aral Sea water use issue more complicated (Zhou et al., 2015; Jiang et al., 2017; Strikeleva et al., 2018).

Land cover is an effective way of investigating the changes caused by complex human and natural interactions (Feddeema et al., 2005; Foley et al., 2005; Feng and Li, 2020). Therefore, the study of land cover dynamics in the basin extent could provide insights into the shrinkage of the Aral Sea as well as its driving factors and impacts to the region (De Beurs et al., 2015; Shen et al., 2019).

Considerable research has been performed to analyze land cover and its dynamics in the Aral Sea basin; however, further engagements are needed to better reveal the land cover change in the basin (Saiko and Zonn, 2000; Löw et al., 2013). Previous studies mainly focused on all of central Asia or small areas around the Aral Sea and the datasets for land cover change were inconsistent and discontinuous (Klein et al., 2012; Kozhoridze et al., 2012; Chen et al., 2013; Hu and Hu, 2019). There has been inadequate research on long-term land cover changes in the Aral Sea basin, particularly in the last 30 years (Lioubimtseva, 2014; De Beurs et al., 2015). In addition, inconsistencies and controversies have been recognized in the findings of many previous land cover studies in the basin, especially regarding the change in cultivated land (Kienzler et al., 2012; Löw et al., 2018; Zhang et al., 2018). Areas of cultivated lands and their distribution are important subjects related to land resources and food security (Conrad et al., 2016; Strikeleva et al., 2018; Liu et al., 2020). It is critical to have a clear understanding of the state of cultivated land in this region. Furthermore, little focus has been paid to the contribution of climate and anthropogenic factors to the shrinking of the Aral Sea starting from the 1990s and going on until today (Berdimbetov et al., 2020).

Here, we analyze the spatiotemporal pattern changes of land cover in the entire Aral Sea basin and its possible driving factors from 1992 to 2015 at a successive annual scale. The annual Climate Change Initiative (CCI) land cover dataset was adopted in the analysis to provide a spatiotemporally consistent delineation of the land cover for the period (Tsendsazar et al., 2015; Yang et al., 2017; Hua et al., 2018; Liang et al., 2019). We attempted to address the following questions: 1) How did the Aral Sea water area change during 1992–2015? 2) How had the

land cover in the extent of the basin been altered during the period, and what effects did the changes, particularly those related to agriculture, contribute to the change of the Aral Sea?

2. Materials and methods

2.1. The Aral Sea basin

The Aral Sea basin (55–75°E, 35–50°N) is located in arid central Asia and has two main river systems: the Syr Darya and the Amu Darya rivers (Shibuo et al., 2007). The total basin area is approximately 1.23 million km² and has a typical continental climate (Huang et al., 2013; Lioubimtseva, 2015). The landform pattern is very simple, mainly consisting of the Turan Plain in the west and mountainous areas in the southeast, and the overall terrain gradually decreases in elevation from the southeast to the northwest (Fig. 1). The average annual precipitation in the basin is approximately 270 mm, with precipitation falling mainly in winter and spring (Chen et al., 2011), and the average temperature is approximately 9 °C (Harris et al., 2014). Over the years, the annual average total runoff in the Aral Sea basin has been approximately 104 km³; the Amu Darya and the Syr Darya flow through the desert and finally into the Aral Sea in the western lowlands (Khan and Holko, 2009). The basin lies within the territorial regions of Kazakhstan, Tajikistan, Uzbekistan, Turkmenistan, Kyrgyzstan, Afghanistan, Iran, and seven other countries (Conrad et al., 2016). The population in the basin is nearly 47 million and is roughly concentrated along river valleys.

2.2. Data sources

2.2.1. Cartographic data

The spatial boundary data of the Aral Sea basin were derived from the revision of hydrological products provided by the Food and Agriculture Organization of the United Nations (FAO) AQUASTAT database (Fig. 1). The elevation data were obtained from the Shuttle Radar Topography Mission (SRTM) data that are measured by the National Aeronautics and Space Administration (NASA) and the National Imagery and Mapping Agency (NIMA). The spatial resolution of the data was 90 m (Li et al., 2017).

2.2.2. CCI-LC data

The Climate Change Initiative-Land Cover (CCI-LC) project is sponsored by the European Space Agency (ESA) and developed a global land cover dataset with 300 m spatial resolution and an annual basis for a period of 24 years from 1992 to 2015 (<http://maps.elie.ucl.ac.be/CCI/viewer/>). The dataset is delivered in a geographic coordinate system (GCS) with a World Geodetic System 84 (WGS84) reference ellipsoid (ESA, 2017). The key aspect of the CCI-LC dataset consists of its consistency over time (Bontemps et al., 2012). Using Envisat MERIS (2003–2012) as a baseline, it makes use of the entire data source of AVHRR (1992–1999), SPOT-VGT (1999–2013), and PROBA-V data for 2013, 2014, and 2015. The typology was defined in 37 original land cover classes complying with the Land Cover Classification System (LCCS) developed by the United Nations (UN) Food and Agriculture Organization (FAO) (Di Gregorio and Jansen, 2005). The accuracy of CCI-LC products was evaluated at a global scale, and the reported overall accuracy reached 79% after independent data verification of ground reference data and substitute sensors (W. Li et al., 2018). The accuracy of

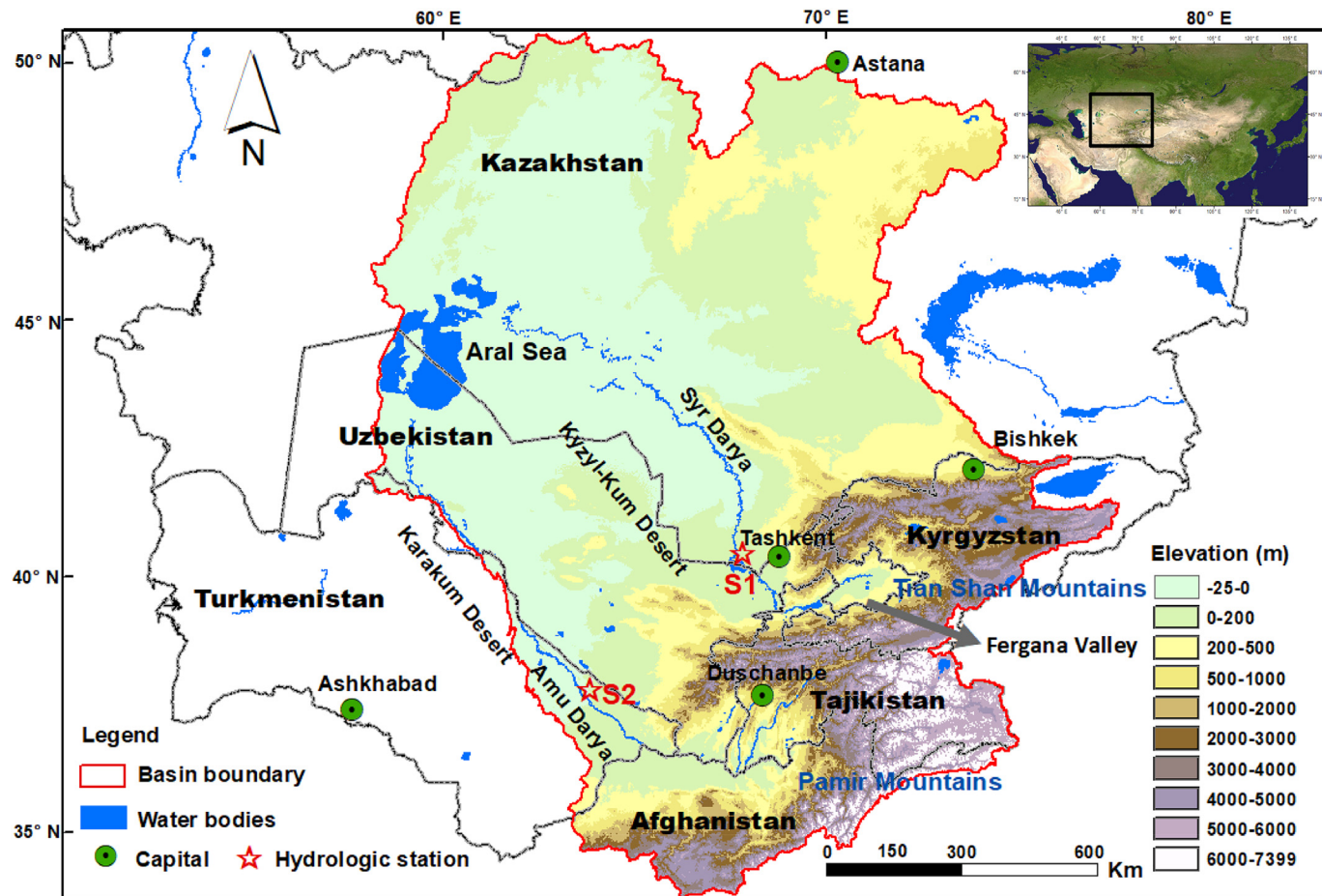


Fig. 1. Geographical map of the Aral Sea basin. S1 and S2 represent the Chinaz River and Kerki River stations, respectively. The figure shows the water bodies in 2002. The inset shows the scope of the box.

the dataset was investigated in central Asia and reported that the CCI-LC has the highest spatial resolution among GLC2000, GlobCover 2009, MODIS land cover datasets and has better accuracy in the study area (Yang et al., 2017; Li et al., 2019).

2.2.3. Meteorological and hydrological data

The monthly temperature (1992–2013) and precipitation (1992–2015) obtained from the Climate Research Unit (CRU), University of East Anglia, were used to analyze climatic variations (http://data.ceda.ac.uk/badc/cru/data/cru_ts/cru_ts_4.00/, reference). The dataset has a spatial resolution of 0.5° (Mitchell and Jones, 2005). The actual daily evapotranspiration (ET) data were published by the Diego Team, University of Ghent, Belgium and are available at <http://www.gleam.eu> (Martens et al., 2017). Based on the Priestley–Taylor formula, the actual evapotranspiration of the global land surface estimated by the Global Land Evaporation Amsterdam Model (GLEAM v3.3a) has a spatial resolution of 0.25° and a temporal resolution of 1 d, spanning from 1992 to 2015 (López et al., 2017; Khan et al., 2018).

2.2.4. Statistic data

Data on crop yields, grazing quantities, and populations in the Aral Sea basin were obtained from the Food and Agriculture Organization (FAO) and mainly included the total population of Kyrgyzstan, Tajikistan and Uzbekistan; the total number of goats, sheep, and horses and the livestock production in these countries; the main crop (wheat, barley, maize, and rice) yields in these countries; and the gross domestic product values of these countries (López et al., 2017; Khan et al., 2018). We only included the

livestock for Kazakhstan because the Aral Sea basin in the country mainly covered by grassland, shrubland, and forests. The cropland of Kazakhstan (10–20 million ha) is much higher than any of other Aral Sea basin countries (<5 million ha) and only a small fraction of the Kazakhstani cropland (<20%) are located in the basin extent. Similarly, only a small fraction of Kazakhstan population is located in the Aral Sea basin. Therefore, the crop area, yield, and population metrics of Kazakhstan were not included in Fig. 6 because of the concern of incomparability between the national-wide metrics of Kazakhstan and the metrics for the Aral Sea basin. The data from 1992 to 2015 are available at <http://www.fao.org/faostat/en/#data/OA>.

Data on the water volume, water surface area, water level of the Aral Sea, and the volume of water delivered to the Aral Sea and water resource distribution were obtained from the Portal of Knowledge for Water and Environmental Issues in Central Asia (CAWATERinfo). Data early start from 1960 and are available at http://www.cawater-info.net/index_e.htm.

2.3. Methods

2.3.1. Land cover reclassification and change detection

To reveal the spatial distributions and temporal transitions of the land covers at a general level, the original CCI land cover types were aggregated to a schema consisting of 8 classes using ArcMap 10.3 (Table 1), including water bodies, cultivated land, forest, sparse vegetation, bare land, wetland, urban land, and others (Wei et al., 2018; Li et al., 2019).

Table 1

Reclassification and description of land cover products.

Reclassification	CCI land cover classification legend	Description
1. Water bodies	210	Water
2. Cultivated land	10, 11, 12	Cropland, rainfed
3. Forest	20	Cropland, irrigated or post-flooding
	30	Mosaic cropland (>50%)/natural vegetation (tree, shrub, herbaceous cover) (<50%)
	40	Mosaic natural vegetation (tree, shrub, herbaceous cover) (>50%)/cropland (<50%)
	50	Tree cover, broadleaved, evergreen, closed to open (>15%)
	60, 61	Tree cover, broadleaved, deciduous, closed to open (>15%)
	70, 71, 72	Tree cover, needle leaved, evergreen, closed to open (>15%)
	80, 81	Tree cover, needle leaved, deciduous, closed to open (>15%)
	90	Tree cover, mixed leaf type (broadleaved and needle leaved)
	100	Mosaic tree and shrub (>50%)/herbaceous cover (<50%)
	170	Tree cover, flooded, saline water
4. Sparse vegetation	110	Mosaic herbaceous cover (>50%)/tree and shrub (<50%)
	120, 122	Shrubland
	130	Grassland
	150	Sparse vegetation (tree, shrub, herbaceous cover) (<15%)
5. Bare land	200	Bare areas
	201, 202	
6. Wetland	180	Shrub or herbaceous cover, flooded, fresh/saline/brackish water
7. Urban land	190	Urban areas
8. Others	220	Permanent snow and ice

To analyze the changes and transitions between the land cover classes, we applied the state transition matrix. State transition refers to the transfer of objective features from one state to another (Sang et al., 2011). The land cover transfer matrix can reflect the structural characteristics of land cover and the transformation status and direction among different types (Pijanowski et al., 2002).

2.3.2. Trend analysis and Mann-Kendall test

In this study, the Mann-Kendall (M-K) test and linear trend analysis were used to analyze the changes in land cover types, climate, and human activity factors. A least-squares linear regression was used for fitting (De Beurs et al., 2015). The slope of the linear trend was calculated as follows:

$$Slope = \frac{n \sum_{i=1}^n x_i y_i - \sum_{i=1}^n x_i \sum_{i=1}^n y_i}{n \sum_{i=1}^n x_i^2 - \left(\sum_{i=1}^n x_i \right)^2} \quad (1)$$

where n is the number of the year; y_i and x_i are the values of the dependent variable and the independent variable (time) in the i th year, respectively.

The nonparametric M-K test is broadly used to explore possible change trends of ecological and hydrological data, with the advantage that there is no specific assumption on data distribution (X.F. Wang et al., 2019). For the sequence $X = (x_1, x_2, \dots, x_n)$, the Mann-Kendall statistic S is given by Eqs. (2) and (3):

$$S = \sum_{i=1}^{n-1} \sum_{k=i+1}^n \text{sign}(x_k - x_i) \quad (2)$$

$$\text{sign}(x_k - x_i) = \begin{cases} 1 & (x_k - x_i) > 0 \\ 0 & (x_k - x_i) = 0 \\ -1 & (x_k - x_i) < 0 \end{cases} \quad (3)$$

where n is the number of samples, and x_i and x_k are time points i and k , respectively. The significance of the trend is calculated using the statistic Z :

$$Z = \begin{cases} (S-1)/\sqrt{\text{Var}(S)} & \text{if } S > 0 \\ 0 & \text{if } S = 0 \\ (S+1)/\sqrt{\text{Var}(S)} & \text{if } S < 0 \end{cases} \quad (4)$$

$\text{Var}(S)$ is the variance of S ; $Z > 0$ represents the increasing trend of the sequence; conversely, it indicates that the sequence shows a downward trend (Mann, 1945; Kendall, 1975). The significance levels of trends were tested with p -values.

2.3.3. Correlation analysis

To further explore the driving factors of land cover, Pearson correlation analysis (r_{xy}) was used to examine the correlation between land

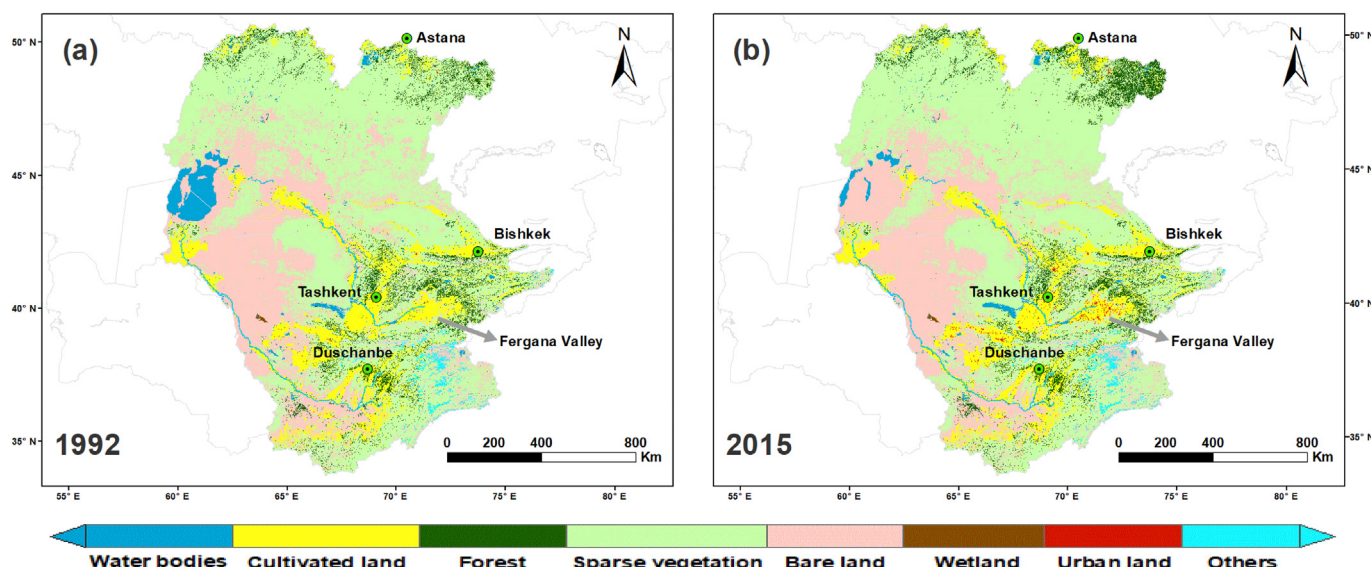


Fig. 2. Land cover spatial distribution of the Aral Sea basin in 1992 (a) and 2015 (b).

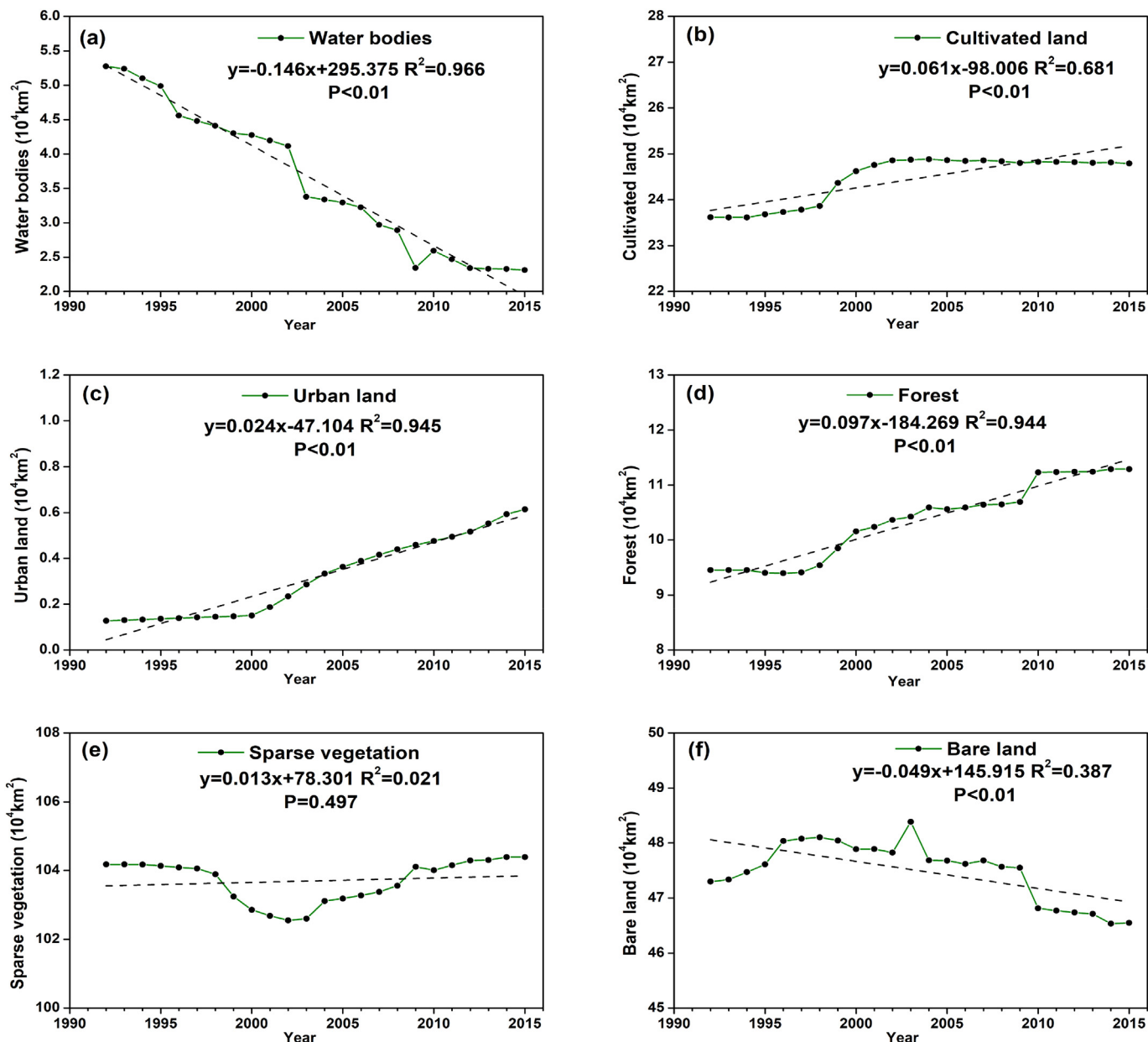


Fig. 3. Changing trends of water bodies (a), cultivated land (b), urban land (c), forest (d), sparse vegetation (e), and bare land (f) during 1992–2015 respectively. $P < 0.01$ indicates a 99% statistical significance level.

cover types and different meteorological and human activity variables (Welford, 1970). All correlation coefficients were between -1 and 1 . A negative correlation means that there is an inverse relationship between variables. Double-tailed values are used to test the significance of these correlations. The formula is as follows:

$$r_{xy} = \frac{\sum_{i=1}^n (x_i - \bar{x})(y_i - \bar{y})}{\sqrt{\sum_{i=1}^n (x_i - \bar{x})^2} \sqrt{\sum_{i=1}^n (y_i - \bar{y})^2}} \quad (5)$$

where n represents the number of samples; x_i and y_i represent the observed values at point i corresponding to variables x and y , respectively; \bar{x} and \bar{y} represent the sample averages of x and y , respectively.

2.3.4. Multiple stepwise regression analysis

Changes in surface elements, such as water bodies, are often related to many factors. To quantitatively describe the influence of each variable on the result, we introduced the multiple stepwise regression method

(Xu et al., 2016). The regression model and the significance test formula are as follows. Suppose the dependent variable Y is dependent on the influence of k independent variables x_1, x_2, \dots, x_n . Then, the structural form of the multiple regression model is:

$$Y = b_0 + b_1 x_1 + b_2 x_2 + \dots + b_k x_k \quad (6)$$

where b_0 is a constant, b_1, b_2, \dots, b_k is called the partial regression coefficient. The F statistic is used to test the trend significance. When F value at the significance level of 0.05, it means that each explanatory variable has a significant impact on the dependent variable.

3. Results

3.1. Land cover distribution in the Aral Sea basin

The land cover types mainly include water bodies, cultivated land, sparse vegetation, and bare land in the basin. The Aral Sea is

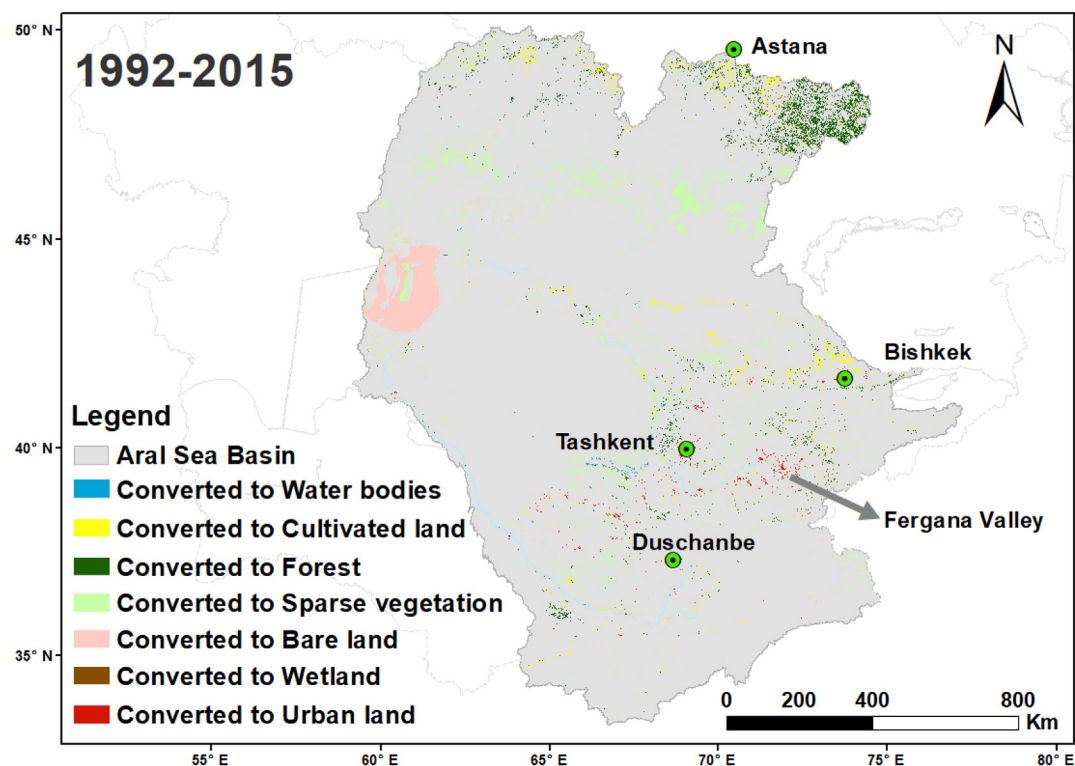


Fig. 4. Land cover type conversion map of the Aral Sea basin from 1992 to 2015.

the largest water body in the basin. The cultivated lands are mainly distributed in the Tashkent, Dushanbe, and Fergana Valley areas, where the majority of the population is located in the basin (Fig. 2). The distribution of forest is relatively random, and most of the distributions are close to the distribution of cultivated land. The sparse vegetation with the largest area is mainly distributed in Kazakhstan, and bare land is concentrated around the lower reaches of Amu Darya. Snow and ice are mainly distributed in the southeast of the basin (Pamir and Tianshan mountains).

3.2. Land cover changes from 1992 to 2015

Spatiotemporal changes in land cover types in the Aral Sea basin are shown in Figs. 3 and 4. From 1992 to 2015, the water area of the Aral Sea decreased at an average rate of $0.146 \times 10^4 \text{ km}^2/\text{year}$ ($p < 0.01$), which was the most significant change in the basin (Fig. 3a). In particular, the southern Aral Sea water area decreased sharply, and 50.38% of the water body areas dried out and were transformed into bare land (Table 2). Although the Aral Sea has shrunk to a large amount of bare land,

Table 2

Transition matrix of land cover change in the Aral Sea basin during 1992–2015. To make the results more reasonable, we averaged the land cover data for each year from 1992 to 1996 (five years) as the starting value in 1992 (horizontal axis) and averaged annual data from 2011 to 2015 (five years) as the end value of 2015 (vertical axis) when creating the transfer matrix. The percentages in parentheses represent the area converted from land type i to land type j as a percentage of the total area of land type i in 1992–2015. The larger values in land cover transfer are shown in bold.

1992/km ² (percent)	2015/km ² (percent)								Sum
	Water bodies	Cultivated land	Forest	Sparse vegetation	Bare land	Wetland	Urban land	Others	
Water bodies	22,297.5 (44.98%)	245.6 (0.50%)	170.0 (0.34%)	1870.9 (3.77%)	24,977.2 (50.38%)	13.0 (0.03%)	1.4 (0.00%)	0	49,575.6 (100.00%)
Cultivated land	177.5 (0.07%)	229,557.3 (96.54%)	529.8 (0.22%)	2893.1 (1.22%)	1975.6 (0.83%)	189.7 (0.08%)	2466.0 (1.04%)	0	237,789.1 (100.00%)
Forest	223.1 (0.23%)	1410.1 (1.44%)	87,637.0 (89.55%)	5672.0 (5.80%)	2492.7 (2.55%)	9.4 (0.01%)	418.8 (0.43%)	0	97,863.1 (100.00%)
Sparse vegetation	204.6 (0.02%)	14,128.9 (1.36%)	25,255.4 (2.43%)	997,014.7 (95.79%)	3579.7 (0.34%)	20.7 (0.00%)	642.3 (0.06%)	0	1,040,846.4 (100.00%)
Bare land	371.3 (0.08%)	2184.3 (0.46%)	744.3 (0.16%)	37,836.7 (8.01%)	430,836.0 (91.26%)	25.2 (0.01%)	111.9 (0.02%)	0	472,109.7 (100.00%)
Wetland	0.1 (0.01%)	0.1 (0.01%)	0	3.0 (0.36%)	0	788.2 (95.98%)	30.0 (3.64%)	0	821.2 (100.00%)
Urban land	0	0	0	0	0	0	1266.7 (100.00%)	0	1266.7 (100.00%)
Others	0	0	0	0	0	0	0	16,599.9 (100.00%)	16,599.9 (100.00%)
Sum	23,274.1 (1.21%)	247,526.2 (44.98%)	114,336.6 (5.96%)	1,045,290.4 (54.53%)	463,861.2 (24.20%)	1046.2 (0.05%)	4937.0 (0.26%)	16,599.9 (0.87%)	1,916,871.7 (100.00%)

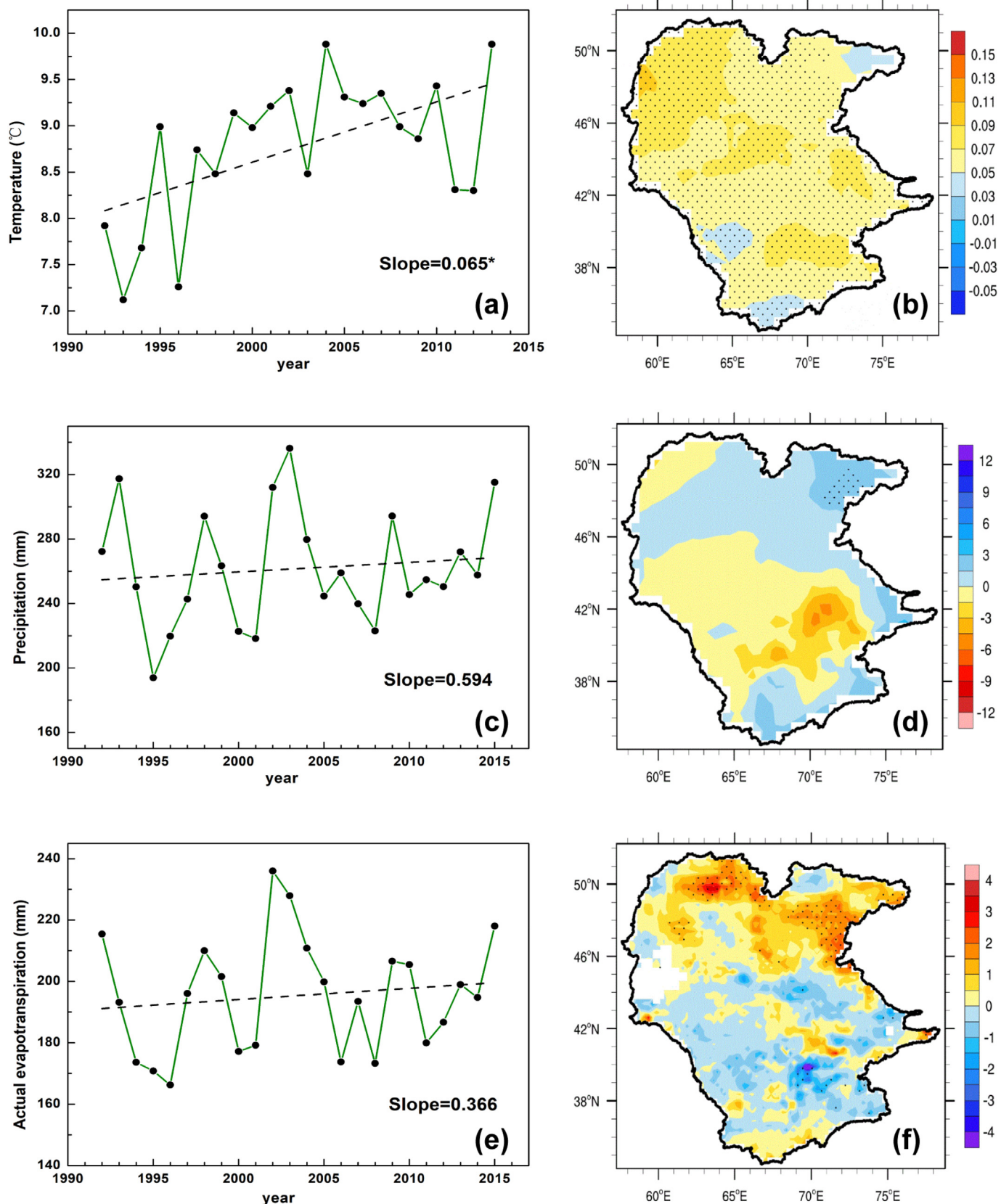


Fig. 5. Spatiotemporal variation in annual temperature, precipitation, and actual evapotranspiration in the Aral Sea basin from 1992 to 2015. The point coverage area indicated was based on a 90% statistical significance level. * represents significant correlations at levels of P -value < 0.05 .

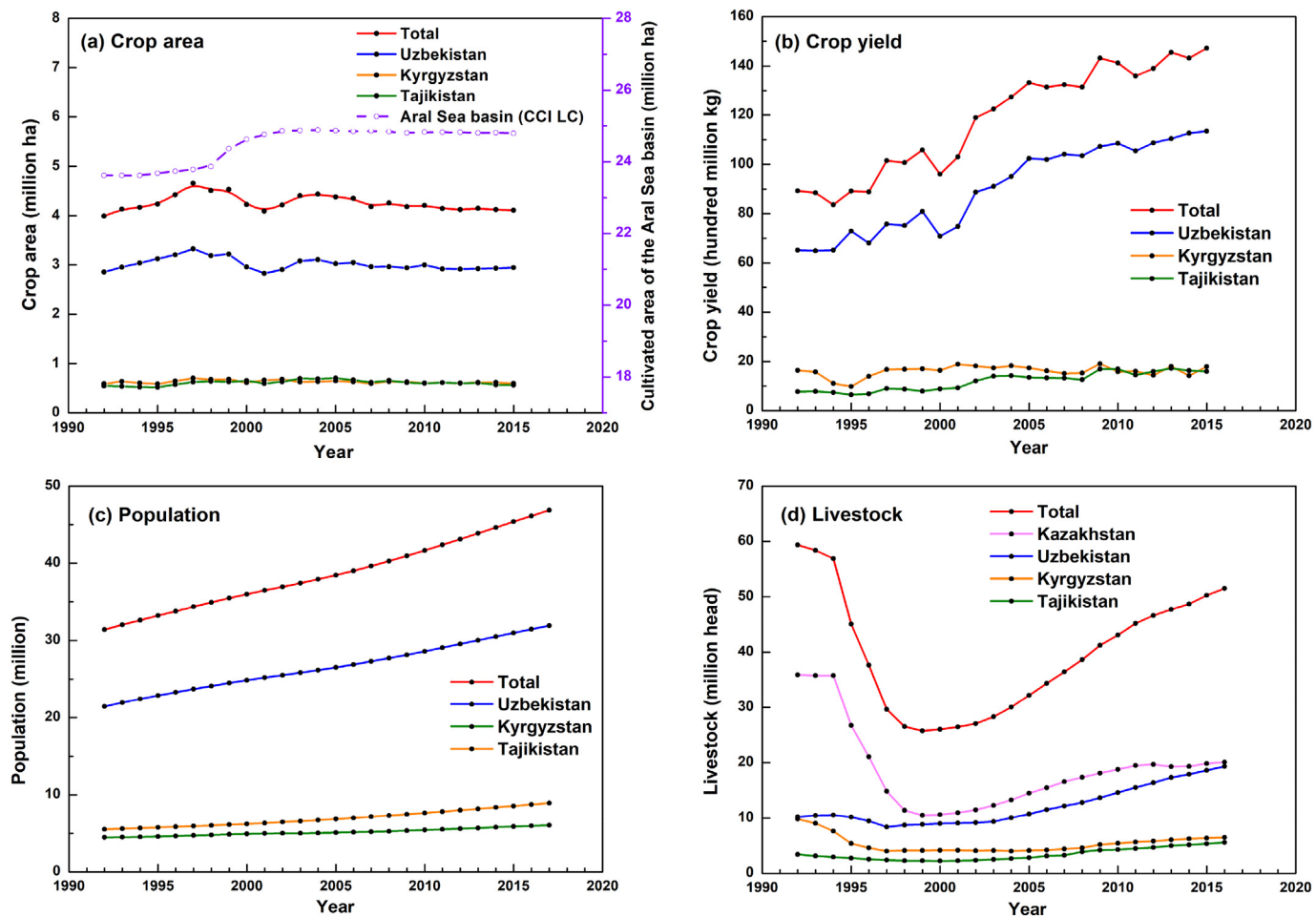


Fig. 6. Annual changes in crop area (a), crop yields (b), population (c), and livestock number (d) in the major countries of the Aral Sea basin (Uzbekistan, Tajikistan, Kyrgyzstan). The data were derived from the FAO (<http://www.fao.org/faostat/en/#data/OA>). The CCI LC derived cultivated land area for the Aral Sea basin over the period is also illustrated in (a) for comparison. We only included the livestock for Kazakhstan because the Aral Sea basin in the country mainly covered by grassland, shrubland, and forests.

approximately 37,836.7 km² of bare land has been converted into sparse vegetation in the north-central part of the basin, resulting in a slight decrease in the area of bare land in the entire basin during 1992–2015 (Fig. 3f).

The area of cultivated land changed from 237,789.1 km² in 1992 to 247,526.2 km² in 2015, with an average growth rate of 0.061×10^4 km²/year ($p < 0.01$) (Fig. 3b). The cultivated land area increased slightly close to Syr Darya, which had the similarity trend of the cropland area reported by the FAO (Fig. 6a), and it was mostly transformed from sparse vegetation. The urban land area increased significantly during the period, with an average rate of 0.024×10^4 km²/year ($R^2 = 0.945, P < 0.01$) (Fig. 3c). Approximately 2466.0 km² of cultivated land in the upper and middle reaches of the basin was developed as urban land as a result of urbanization processing in the region, but the areas were relatively small (1.04%) and insignificant when compared to the total cultivated areas. Despite these area losses, the total cultivated land area was stable with a slightly increasing trend over the 24 years (Fig. 4).

It also reported that approximately 25,255.4 km² of spare vegetation in the northeast part of the basin was transformed into forest (Table 2). The wetland area is small, and the change is insignificant (Fig. 2).

3.3. The effect of climate and human activities on land cover change

3.3.1. Changes in climate variables

Fig. 5 shows the interannual variations of the spatiotemporally averaged climate variables of temperature, precipitation, and actual

evapotranspiration in the Aral Sea basin over the period of 1992–2015. The annual mean temperature indicated a significant increasing trend at a rate of 0.065 °C/year ($P < 0.05$), and the whole area was uniformly significant (Fig. 5a). Precipitation and actual evapotranspiration fluctuated and slightly increased at rates of 0.594 mm/year and 0.366 mm/year (Fig. 5c, e); specifically, they increased significantly in the vegetated area adjacent to the northern part of the basin (Fig. 5d, f).

Generally, climatic warming and drying trends were found in the Aral Sea basin. Furthermore, these results suggested that reduced precipitation in the bare land areas and increased temperature caused an increased water deficit, while water conditions were slightly better in the northern vegetated areas because there was more precipitation (Figs. 2, 5b, d, f).

3.3.2. Changes in human activities

As shown in Fig. 6, we selected crop area, crop yield, population, and livestock number to represent human activities. The cropland area of the major countries in the Aral Sea basin was relatively stable from 1992 to 2015, which was consistent with the change of cultivated land on the whole (Fig. 6a). In addition, the improvement of tillage efficiency is beneficial to the increase in crop yield (Fig. 6b). Uzbekistan's population has increased significantly (Fig. 6c). Livestock number has increased slightly in all countries except Kazakhstan, where there was an inflection point near 2000 (Fig. 6d).

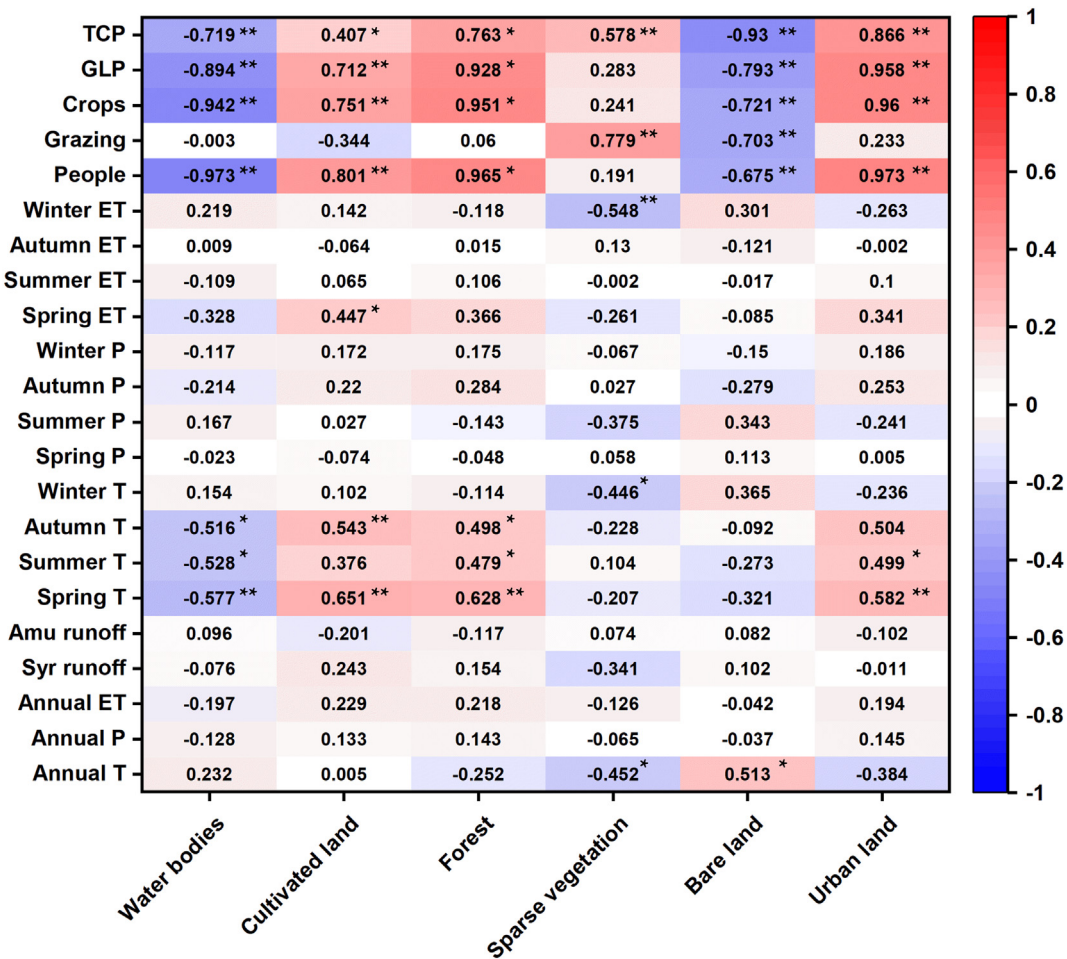


Fig. 7. Pearson's linear correlations between land cover types, climate and human activity factors from 1992 to 2015. T-Temperature; P-Precipitation; ET-Actual evapotranspiration; People-Total population; Grazing-Total quantity of goats, horses, and sheep; Crops-Total production of barley, wheat, corn, and rice; GLP and TCP represent the gross domestic product of livestock and crops, using 2004–2006 as a benchmark value of 100. Significant correlations of $P < 0.05$ (*) and $P < 0.01$ (**) are displayed.

3.3.3. Attribution analysis of land cover change

To explore the relationship between different land cover types, climate, and human activity factors, correlation analysis was conducted, and the results are shown in Fig. 7. All data satisfy the parameter assumption of normal distribution. These results suggested that the variation in surface land cover type area may be more closely related to human activity factors, which indicates the high consistency of the variation to a large extent. There is no doubt that changes in urban land areas and cultivated land areas that are directly controlled by human activities are more closely related to human beings (Fig. 7b, f). However, as the largest water body in the basin and had experienced nearly all of the water area loss in the basin, Aral Sea water change may be affected by both climate and human activities and require more in-depth research. Therefore, the contribution of the influencing factors to the changes in the Aral Sea water area is further discussed using a multiple stepwise regression model (Table 3).

Considering the possible effects on the Aral Sea, climate independent variables include temperature (T) and precipitation (P), human activity variables include population, crop yield, livestock number. In addition,

we added cultivated land and urban land that may have a potential impact on the water body into independent variables.

The regression results show that urban and cultivated land has a significant negative relationship with the Aral Sea, with coefficients of 23.085 and 4.152 respectively ($p < 0.01$). Population increase has a slightly negative effect on the Aral Sea. In addition, the effect of rising temperature on the Aral Sea was insignificant, with a coefficient of only 0.003. The fitting result is satisfactory ($R^2 = 0.984$, P -value < 0.05), and the results indicate that human activities are the main factors for the shrinking of the Aral Sea, and the influence of climatic factors such as temperature and precipitation is small (Table 3).

4. Discussion

4.1. Continued shrinking of the Aral Sea

The Aral Sea is the largest water body in the basin and has experienced nearly all of the water area loss in the basin (Figs. 3a, 4). Our results show that the Aral Sea continued decreasing in recent years

Table 3

Multiple stepwise regression analysis of Aral Sea water area. ** represents significant correlations at levels of P -value < 0.01 .

Multiple stepwise regression model	R^2	F-value	P-value
Aral Sea water area = $-23.085\text{urban}^{**} - 4.152\text{cultivated}^{**} - 0.945\text{population}^{**} - 0.333\text{T} + 167.917$	0.984	7.412	0.014

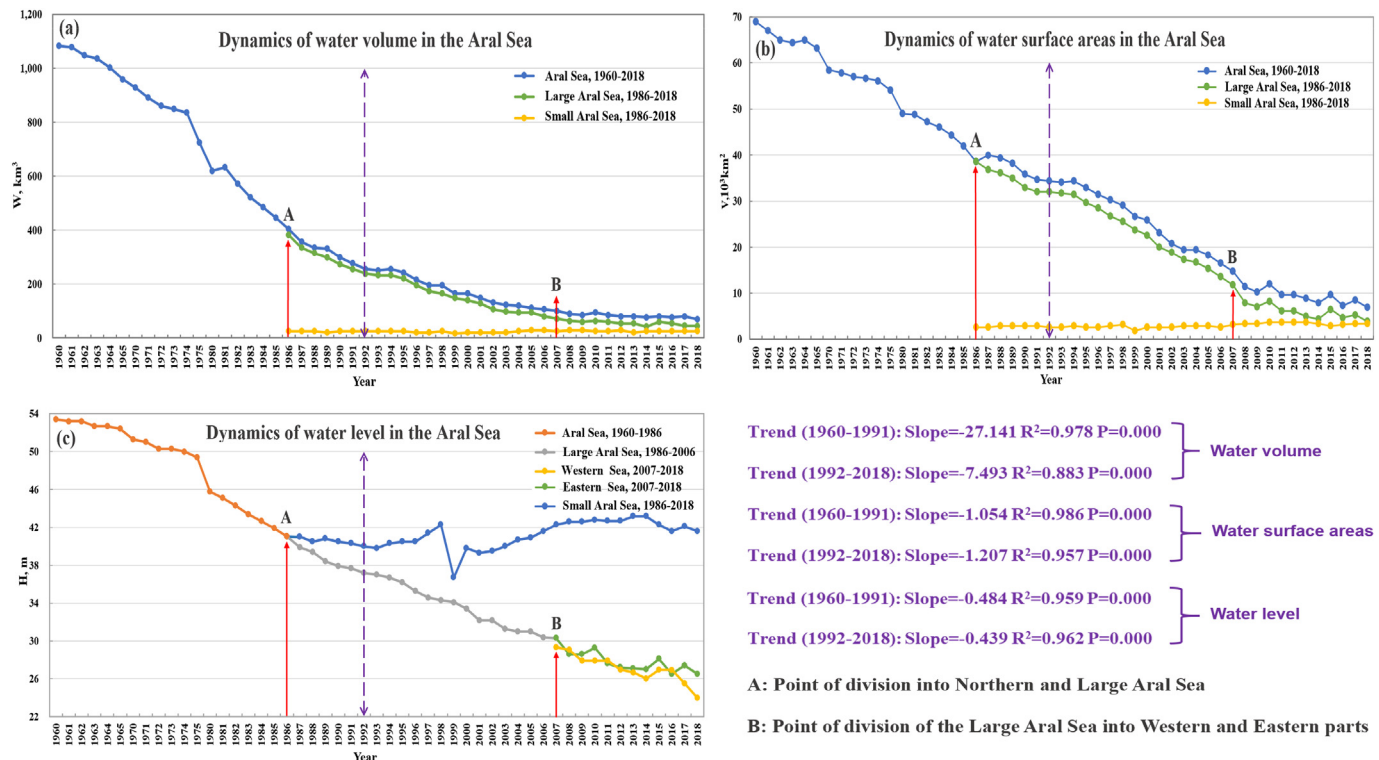


Fig. 8. Changes in the volume (a), surface area (b), and water level (c) of the Aral Sea from 1960 to 2018. A is the point of division into the northern and large Aral Sea; B is the point of division of the large Aral Sea into western and eastern parts. The variation in the Aral Sea before and after 1992 was compared. The data were derived from the CAWATERinfo (http://www.cawater-info.net/index_e.htm).

(Fig. 8). From 1992 to 2018, the water volume and water level in the Aral Sea decreased at rates of $7.493 \text{ km}^3/\text{year}$ and 0.439 m/year respectively. This was relatively slow compared with the period from 1960 to 1991 (Fig. 8a, c). The Aral Sea water surface areas decreased slightly

faster after 1992 than before (Fig. 8b). Overall, the average rate of decline is lower than in the Soviet era (Spoor, 1998; Micklin, 2016; Zou et al., 2019). However, the exact reason for the continued decline is still unknown (Wang et al., 2020).

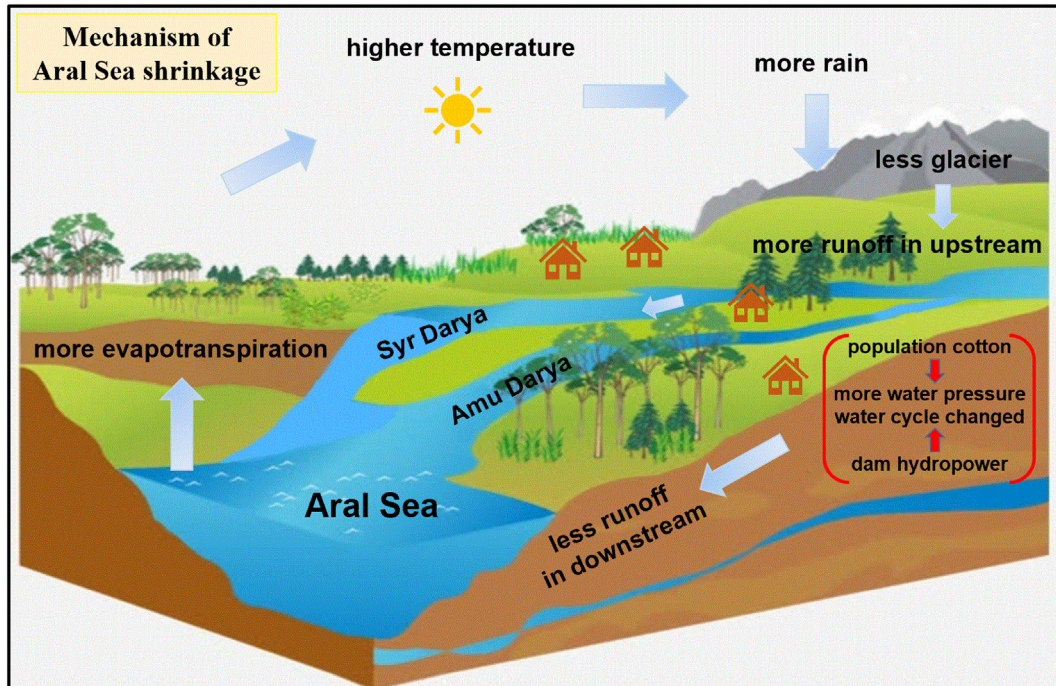


Fig. 9. Framework of the mechanism of Aral Sea shrinkage.

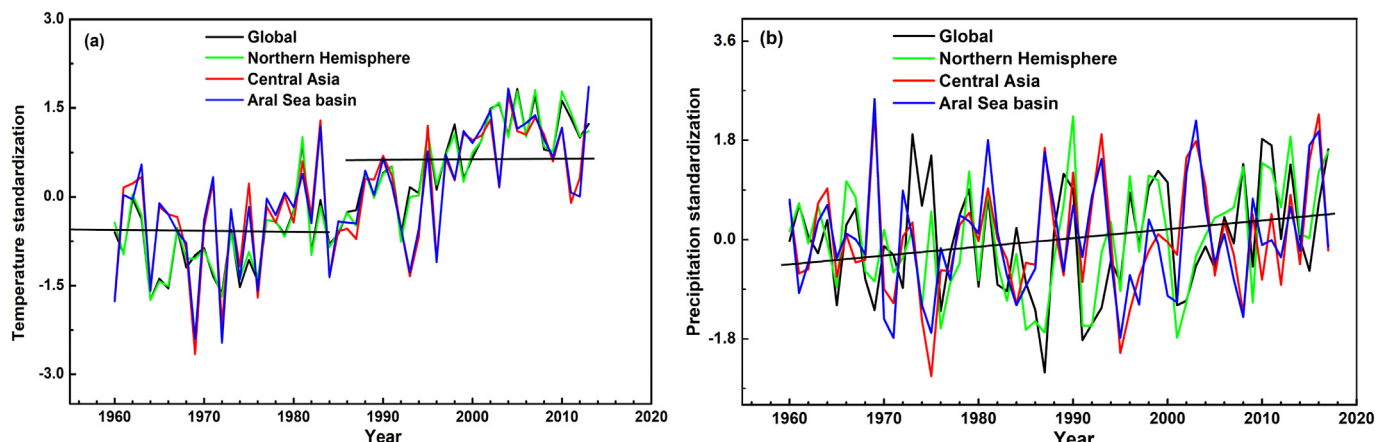


Fig. 10. Standardized changes in temperature (a) and precipitation (b) from 1960 to 2015. Four scales of global, northern hemisphere, central Asia, and Aral Sea basin are selected for measurement.

The shrinkage of the Aral Sea started in the 1960s and its volume decreased approximately 800 km³ by 1992 (Fig. 8a). In 1986, the Aral Sea was divided into the South Aral Sea and the North Aral Sea (Zhang et al., 2019). The North Aral Sea was stabilized through the construction of a hard wall dam completed in 2005 (Fig. 8b, c) (Micklin, 2004; Massakbayeva et al., 2020). Around 2007, the South Aral Sea was completely divided into the east basin and the west basin, and the water level in the west basin dropped significantly (Fig. 8c) (Lioubimtseva, 2014; Shi et al., 2014). The exposure of the surface to bare land increases the ecological risk of the surrounding area, resulting in the heating of air, aggravation of sand and dust, and desertification, which will have irreversible consequences on the ecological environment (Small et al., 2001; Micklin et al., 2014).

Agricultural activities have been considered an important factor affecting the shrinkage of the Aral Sea since the 1960s (Micklin, 1992; Micklin, 2016); therefore, what changes have occurred in the agricultural area in the post-Soviet era, and has there been a significant expansion that has caused the Aral Sea to shrink further?

4.2. Cultivated land increased slightly in the post-Soviet era

Primarily, there has been much controversy over the area of cultivated land in the Aral Sea basin (Kienzler et al., 2012; Chen et al., 2013; Zhang et al., 2018). The inconsistency is mainly reflected in the following two aspects: (1) the cultivated land areas derived from statistical data and early remote sensing products (such as MODIS land cover products) were found to be very inconsistent (Fritz and See, 2008; Li et al., 2019). The cultivated land area reported by early remote sensing is generally slightly higher than the statistical data (Chen et al., 2018; Li et al., 2019); and (2) the area of changed cultivated land reported by remote sensing datasets also shows different changing trends. For example, the farmland areas obtained by MODIS and the CCI-LC products are opposite (Chen et al., 2013). According to MODIS data, the area of cultivated land in the Aral Sea basin decreased by approximately 18.1 thousand km² between 2000 and 2010, while the CCI-LC results indicated relative stability, with a slight increase of 2000 km² (Klein et al., 2012). This may be due to many factors, e.g., the classification schemes,

classification method, connotation of land use types, and resolution size result in inconsistencies among land-cover datasets (Hua et al., 2018). Other researchers have also concluded that MODIS and CCI land cover products have inverse time series trends elsewhere (Fritz et al., 2011; Liu et al., 2019; L. Wang et al., 2019).

Our results and various sources show that cultivated land was relatively stable in the Aral Sea basin in the post-Soviet era. These sources include the CAWATERinfo website, which is a portal of knowledge for water and environmental issues in central Asia, the cropland area statistics from FAO (Food and Agriculture Organization of the United Nations) (Fig. 6a), the Soviet Statistical Yearbook (data after 2000), and the GlobeLand30 (high resolution: 30 m) products, which is a high-resolution land cover product for 2000 and 2010 (Chen et al., 2018; Liang et al., 2019; Liu et al., 2020). In general, it has been demonstrated that the newly released annual CCI-LC data not only provide continuous and long-term land cover sequences but are more accurate in many areas (for example, Tsendbazar et al., 2015; Yang et al., 2017; Liang et al., 2019).

We believe that MODIS land cover products have a biased description of cultivated land in this region, and our results indicate that the concept of relatively stable and insignificant expansion of cultivated land in the Aral Sea basin is trustworthy. Moreover, we question the conclusion that there was large-scale abandoned farming in the post-Soviet era (Chen et al., 2013; Klein et al., 2012; Hua et al., 2018).

4.3. Interpretation of the driving factors of the Aral Sea shrinkage

Climate, hydrology, ecosystems, and human activities in the Aral Sea basin are tightly interconnected (Lioubimtseva, 2014). On a regional scale, the allocation of water resources in the upper, middle, and lower reaches of the basin determines the water area of the Aral Sea (X. Li et al., 2018; Massakbayeva et al., 2020). The analysis of Aral Sea dynamics is shown in Fig. 9. As a closed inland lake, the inflow of the Aral Sea mainly depends on the runoff of the Syr Darya and Amu Darya (which is the main tributary of the Aral Sea and accounts for approximately 68% of the total runoff entering the Aral Sea basin (Singh et al., 2012; Hagg and Bolch, 2015)), originating from the Pamir and

Table 4

Results of Mann-Kendall trend test performed for climatic and hydrological factors. T-temperature; P-precipitation; AET-actual evapotranspiration; STS and ATS represent water delivery to the Aral Sea from the Syr Darya basin and Amu Darya basin, respectively.

Data	T	P	AET	Kizilshlak	Nijnii	Chinaz	Kerki	STS	ATS
Z	2.343	0.719	0.670	2.655	0.395	-0.634	-1.017	-0.691	-1.752
P-value	0.019	0.472	0.503	0.008	0.693	0.526	0.309	0.489	0.080

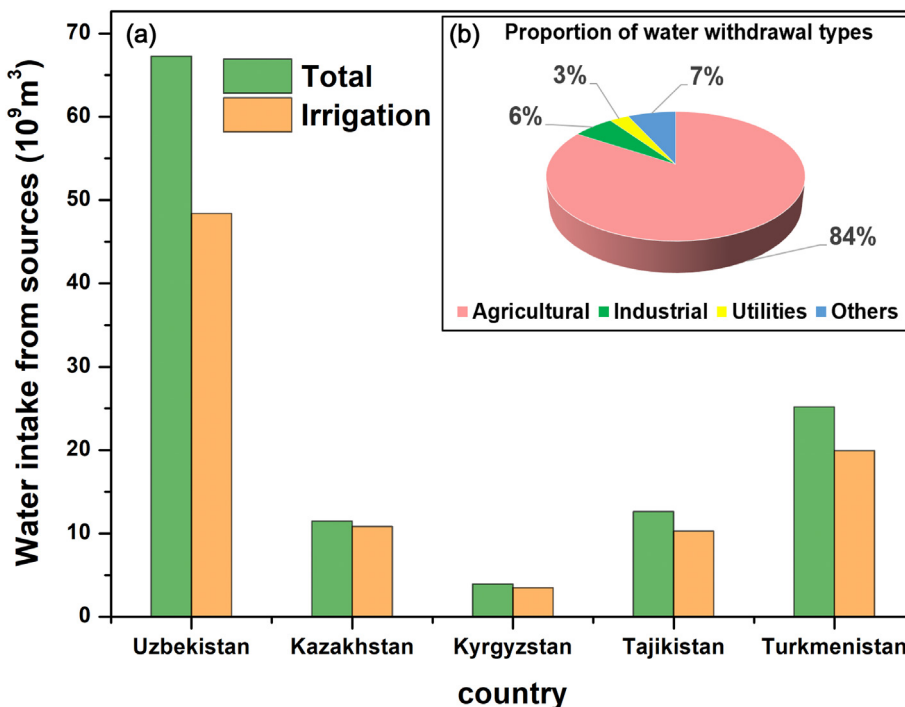


Fig. 11. Water volume of each country draws from its source (a) and proportion of water withdrawal types (b) in Aral Sea basin. The average data from 1980 to 1995 represents the status and distribution of the overall water intake.

Tianshan mountains in the upper reaches (Lioubimtseva, 2015; Chen et al., 2018). The expenditure is mainly lake evaporation (Micklin and Aladin, 2008; Singh et al., 2012).

Since the middle of the 20th century, meteorological data have shown that there has been a stable and significant warming trend in both the large-scale global and the small-scale Aral Sea basin (Li et al., 2015; Huang et al., 2017), and the changes in the Aral Sea basin have been more prominent (Fig. 10a). Our results showed that from 1992 to 2015, the temperature of the Aral Sea basin gradually increased at an average rate of approximately 0.065 °C/year ($P < 0.05$) (Table 4). Climate warming is more significant in mountainous areas, and the main manifestations are the rapid increases in air temperature, precipitation increases, and rapid changes in the mountain cryosphere (Hagg et al., 2013; Chen et al., 2016; X. Li et al., 2018). These phenomena lead to the increased runoff in the upper reaches of the Amu Darya and Syr Darya (Fig. 12a, b) and are favorable factors to alleviate water scarcity in the basin (Khan and Holko, 2009; Chen et al., 2018).

However, the large water supply demand in the middle and upper reaches and the lake evapotranspiration enhanced by climate warming have negative effects on the Aral Sea (Micklin and Aladin, 2008; Massakbayeva et al., 2020). Our results showed that the shrinking of the Aral Sea in the post-Soviet era is significantly negatively correlated with human activities such as agriculture and urban expansion (Table 3; Fig. 7a). The water used by human activities mainly includes the water drawn by agriculture, industry, and cities in the basin (Fig. 11), among which agriculture is the largest water consuming sector (about 84% of total water consumption, see Fig. 11a) and has long been considered to be the chief culprit for shrinking the Aral Sea (Shibuo et al., 2007; Zou et al., 2019). Before 1992, the Aral Sea was threatened by a massive increase in irrigated farmland in the basin (Micklin, 2010; Lioubimtseva, 2014). Our results show that the scale of cultivated land only increased slightly during 1992–2015 (Figs. 3b, 4, 6a); however, high correlation was found between the changes of the cultivated land and the water extent of the Aral Sea (Table 3), suggesting that the agricultural water consumption continued to contribute

to the shrinkage of the Aral Sea. The same conclusions were also reported by Li et al. (2021) and Liu et al. (2020). Therefore, the Aral Sea was still shrinking because large areas of farmland remain and had exceeded the tolerance of the Aral Sea. High farmland water demand continued to exert the influence that existed during the Soviet era (Lioubimtseva, 2015; Conrad et al., 2016). In addition, the massive increase in the urban population led to the acceleration of urbanization, such as in Tashkent and Dushanbe, which are the major cities in the basin (Fig. 6c). Studies have shown that urbanization in these cities increased the amount of water used for human production and living (Luan and Li, 2021). However, the proportion of urban land cover is rare, and the utilization of water resources is far less than that of agricultural water consumption (84%), but it has a slight aggravating effect on the whole (Fig. 11b).

Excessive farmland water use and insufficient water supply to the Aral Sea persisted in the post-Soviet era, especially in the Amu Darya basin. From 1992 to 2019, the rate of decrease of the water delivery to the Aral Sea from the Amu Darya basin was 0.434 km³/year, which was much higher than that of the Syr Darya basin to the Aral Sea (Fig. 13a, b). Downstream runoff site data also showed a significant reduction in Amu Darya runoff (Fig. 12d, the decreasing rate is 0.318 km³/year). The loss of water in the Amu Darya basin is the direct cause of the Aral Sea's shrinkage (Wang et al., 2016). Specific manifestations include Uzbekistan's cotton cultivation and alternative water supply measures consuming approximately 52% of the water from the Amu Darya (Fig. 11a) (Micklin and Aladin, 2008; Liu et al., 2020; Ruan et al., 2020); Turkmenistan has diverted approximately 20% of the water from the Amu Darya into the Karakum Canal to irrigate farmland (Allouche, 2007; Micklin et al., 2014; Strikeleva et al., 2018). Other factors such as the construction of large hydropower stations and reservoirs, including the Tuyamuyun Reservoir (near the entrance to the lower Amu Darya), Toktogul Reservoir (an immense water conservancy project in the upper reaches of the Syr Darya), and Rogun Dam (located in Tajikistan and restored in 2008), have exacerbated the effect (Eshchanov et al., 2011; Li et al., 2017; Zhou et al., 2019).

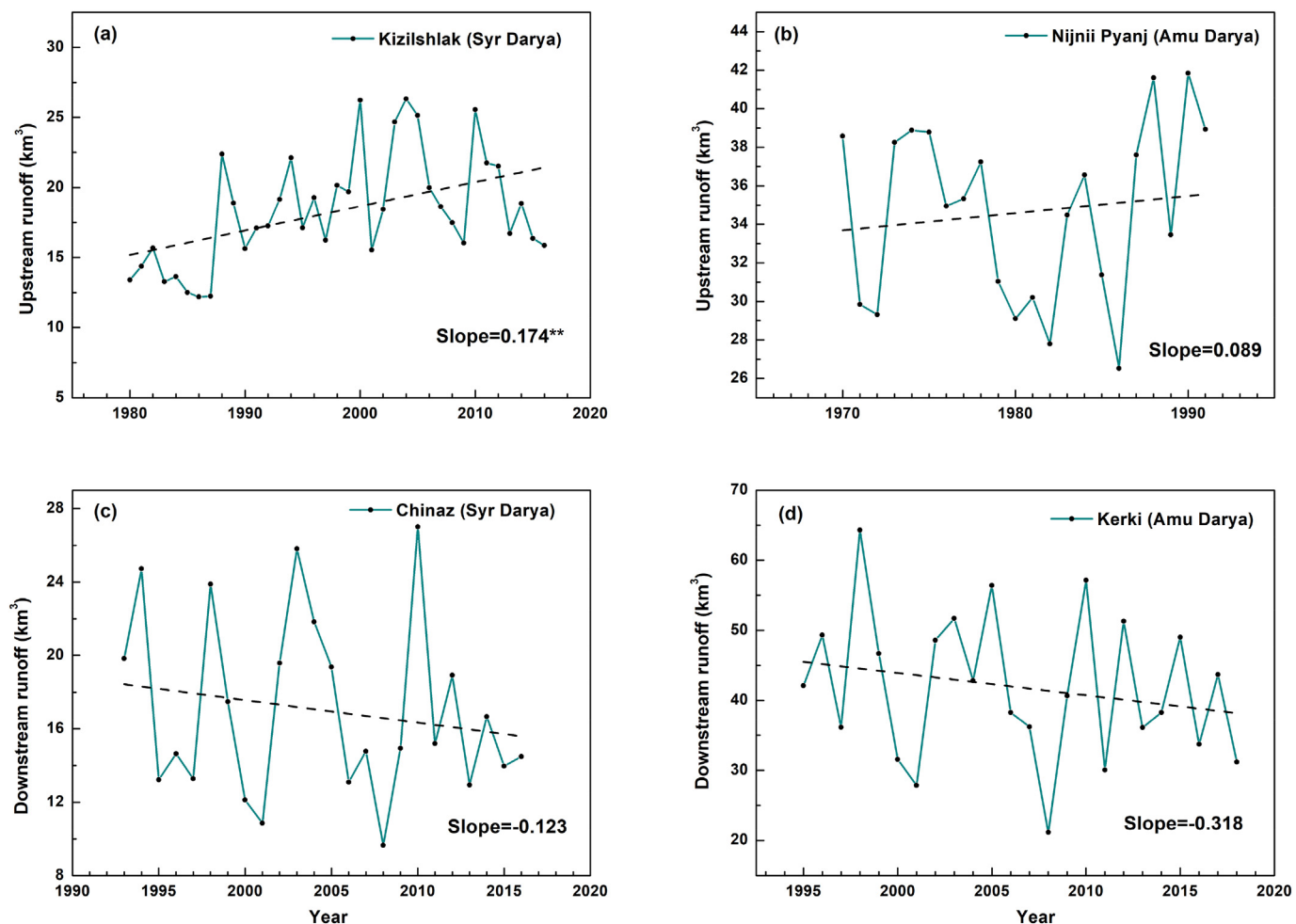


Fig. 12. Annual runoff changes (km^3/year) in the upper and lower reaches of the Syr Darya and Amu Darya basins were collected. The upstream sites were the Kizilshlak River (40.29°N , 69.75°E) and Nijnii Pyanj River (37.19°N , 68.59°E), which are runoff series of mountain exit stations. The downstream sites were the Chinaz River (40.94°N , 68.76°E) and Kerki River (38.38°N , 65.42°E). ** represents significant correlations at levels of P -value < 0.01 .

Overall, climate change has a positive effect on the water supply of the Aral Sea, and the Aral Sea is still shrinking largely because high water consumption of agriculture continues to exert the influence that existed during the Soviet era. Other reasons, such as the increased

water demand for urbanization have exacerbated this effect. The amount of water flowing into the Aral Sea is insufficient to maintain the existing water surface and is lost continuously every year (Singh et al., 2012; Shi et al., 2014).

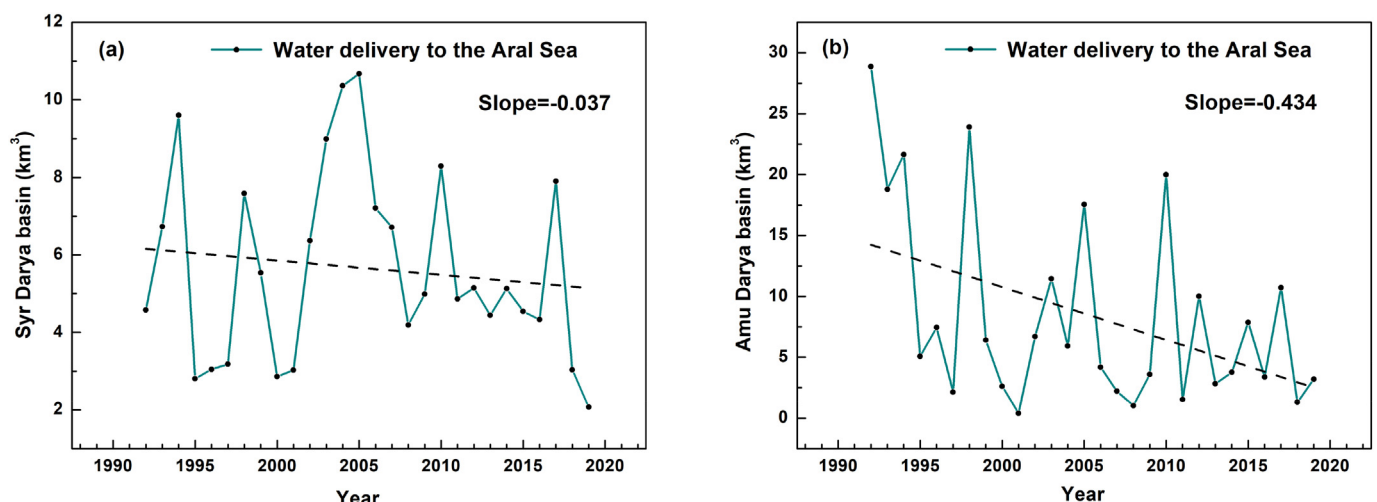


Fig. 13. Volume changes of water delivery to the Aral Sea (km^3) from the Syr Darya basin (a) and Amu Darya basin (b) during 1992–2018. * represents significant correlations at levels of P -value < 0.05 .

4.4. Limitations and future work

CCI-LC is a medium-resolution land cover product, and its annual temporal resolution provides the ability to detect the trend of land cover changes, especially the general land cover classes in a large region. However, limited by its spatial precision, it could not accurately represent the detailed spatial structure of certain land cover types and their changes over time (Yang et al., 2017). The aggregation of the land cover classes applied in the analysis could reduce the impacts from the uncertainties for the detailed classes (Fritz and See, 2008; W. Li et al., 2018), but it limited the analysis to only the transitions among the general classes. The current analysis presumed that the water consumption for agriculture and urbanization is linearly related to their area, and further analysis could be conducted to investigate and adjust the relationship. More work could be done to better reveal the changes in ecosystems and human activities, such as the shift in planting crops, and their contributions to the shrinkage of the Aral Sea.

Aral Sea shrinkage is a complex process involving water circulation (Li et al., 2019). It would be very interesting to produce land cover data for an expanded time frame and conduct more in-depth analysis for a longer or even the full time frame of the Aral Sea shrinkage in the future.

5. Conclusions

This paper analyses the dynamics of land cover during 1992–2015 and its driving factors in the Aral Sea basin based on the continuous and consistent long-term CCI-LC sequence combined with hydroclimatic and human activity data, with a particular focus on the shrinking of the Aral Sea and the change of cultivated land. We conclude the following:

- (1) In recent years, the water area in the Aral Sea had been continuously decreasing every year but at a slower rate than during the Soviet times, and approximately 50.38% of its water area in 1992 dried out and turned into bare land by 2015. The relative stability with a slight increase in the cultivated land area leads us to firmly believe that there was no large-scale abandoned or expanded agriculture in the post-Soviet era.
- (2) The impact of farmland irrigation on the shrinkage of the Aral Sea could be traced back to the 1960s. From 1992 to 2015, the area of cultivated land was relatively stable. Climate change had a positive effect on the water supply of the Aral Sea, and the Aral Sea is still shrinking largely because high water consumption of agriculture continues to exert the influence that existed during the Soviet era. Other factors, such as the increased water demand for urbanization has exacerbated this effect, making the amount of water flowing into the Aral Sea insufficient to maintain the existing water surface and continuing to be lost every year.

This work provides a useful reference for local managers and government departments when making decisions and for understanding land cover change in the Aral Sea basin.

CRediT authorship contribution statement

This is the only submission of this manuscript and no parts of this manuscript are being considered for publication elsewhere. All authors have approved this manuscript and the submission. No author has financial or other contractual agreements that might cause conflicts of interest.

Declaration of competing interest

All authors have approved this manuscript and the submission. The authors declare no conflicts of interest. The funding sponsors had no role in the design of the study; in the collection, analyses, or

interpretation of data; in the writing of the manuscript, or in the decision to publish the results.

Acknowledgments

This research was supported by the National Key Research and Development Program of China [grant number 2018YFA0606404], the National Natural Science Foundation of China [grant number 41988101] and the National Natural Science Foundation of China [grant number U1803341].

References

- Allouche, J., 2007. The governance of Central Asian waters: national interests versus regional cooperation. *Central Asia at the Crossroads*. 4, pp. 46–55.
- Bekchanov, M., Ringler, C., Bhaduri, A., Jeuland, M., 2016. Optimizing irrigation efficiency improvements in the Aral Sea basin. *Water Resour. Econ.* 13, 30–45. <https://doi.org/10.1016/j.wre.2015.08.003>.
- Berdimbetov, T.T., Ma, Z.G., Liang, C., Ilyas, S., 2020. Impact of climate factors and human activities on water resources in the Aral Sea basin. *Hydrology* 7 (30), 1–14. <https://doi.org/10.3390/hydrology7020030>.
- Bontemps, S., Herold, M., Kooistra, L., Van Groenestijn, A., Hartley, A., Arino, O., Moreau, I., Defourny, P., 2012. Revisiting land cover observation to address the needs of the climate modeling community. *Biogeosciences* 9, 2145–2157. <https://doi.org/10.5194/bg-9-2145-2012>.
- Chen, F.H., Huang, W., Jin, L.Y., Chen, J.H., Wang, J.S., 2011. Spatiotemporal precipitation variations in the arid Central Asia in the context of global warming. *Sci. China Earth Sci.* 54 (12), 1812–1821. <https://doi.org/10.1007/s11430-011-4333-8>.
- Chen, X., Bai, J., Li, X.Y., Luo, G.P., Li, J.L., Li, B.L., 2013. Changes in land use/land cover and ecosystem services in Central Asia during 1990–2009. *Curr. Opin. Environ. Sustain.* 5 (1), 116–127. <https://doi.org/10.1016/j.cosust.2012.12.005>.
- Chen, Y.N., Li, W.L., Deng, H.J., Fang, G.H., Li, Z., 2016. Changes in Central Asia's water tower: past, present and future. *Sci. Rep.* 6, 35458. <https://doi.org/10.1038/srep35458>.
- Chen, Y.N., Li, Z., Fang, G.H., Li, W.H., 2018. Large hydrological processes changes in the transboundary rivers of Central Asia. *J. Geophys. Res. Atmos.* 123, 5059–5069. <https://doi.org/10.1029/2017JD028184>.
- Conrad, C., Schönbrodt-Stitt, S., Löw, F., Sorokin, D., Paeth, H., 2016. Cropping intensity in the Aral Sea basin and its dependency from the runoff formation 2000–2012. *Remote Sens.* 630 (8), 1–26. <https://doi.org/10.3390/rs8080630>.
- De Beurs, K.M., Henebry, G.M., Owsley, B.C., Sokolik, I., 2015. Using multiple remote sensing perspectives to identify and attribute land surface dynamics in Central Asia 2001–2013. *Remote Sens. Environ.* 170, 48–61. <https://doi.org/10.1016/j.rse.2015.08.018>.
- Di Gregorio, A., Jansen, L.J.M., 2005. *Land Cover Classification System (LCCS): Classification Concepts and User Manual*. Food and Agriculture Organization of the United Nations.
- ESA, 2017. Land Cover CCI Product User Guide Version 2.0. [online] Available from: http://maps.elie.ucl.ac.be/CCI/viewer/download/ESACCI-LC-Ph2-PUGv2_2.0.pdf.
- Eshchanov, B.R., Stultjes, M.G.P., Salaev, S.K., Eshchanov, R.A., 2011. Rogun dam-path to energy Independence or security threat? *Sustainability* 3, 1573–1592. <https://doi.org/10.3390/su3091573>.
- Feddema, J.J., Oleson, K.W., Bonan, G.B., Mearns, L.O., Buja, L.E., Meehl, G.A., Washington, W.M., 2005. The importance of land-cover change in simulating future climates. *Science* 310 (5754), 1674–1678. <https://doi.org/10.1126/science.1118160>.
- Feng, M., Li, X., 2020. Land cover mapping toward finer scales. *Sci. Bull.* 65 (19), 1604–1606. <https://doi.org/10.1016/j.scib.2020.06.014>.
- Foley, J.A., DeFries, R., Asner, G.P., Barford, C., Bonan, G., Carpenter, S.R., Chapin, F.S., Coe, M.T., Daily, G.C., Gibbs, H.K., Helkowski, J.H., Holloway, T., Howard, E.A., Kucharik, C.J., Monfreda, C., Patz, J.A., Prentice, C., Ramankutty, N., Snyder, P.K., 2005. Global consequences of land use. *Science* 309 (5734), 570–574. <https://doi.org/10.1126/science.1111772>.
- Fritz, S., See, L., 2008. Identifying and quantifying uncertainty and spatial disagreement in the comparison of Global Land Cover for different applications. *Glob. Chang. Biol.* 14 (5), 1057–1075. <https://doi.org/10.1111/j.1365-2486.2007.01519.x>.
- Fritz, S., See, L., McCallum, I., Schill, C., Obersteiner, M., Van der Velde, M., Boettcher, H., Havlik, P., Achard, F., 2011. Highlighting continued uncertainty in global land cover maps for the user community. *Environ. Res. Lett.* 6 (044005), 1–6. <https://doi.org/10.1088/1748-9326/6/4/044005>.
- Hagg, W., Bolch, T., 2015. Less water from the mountains? Consequences of glacier changes in Central Asia. *Environmental Crises in Central Asia*. Routledge, pp. 31–42 <https://doi.org/10.5167/uzh-129185>.
- Hagg, W., Hoelzle, M., Wagner, S., Mayr, E., Klose, Z., 2013. Glacier and runoff changes in the Rukhk catchment, upper Amu-Darya basin until 2050. *Glob. Planet. Chang.* 110, 62–73. <https://doi.org/10.1016/j.gloplacha.2013.05.005>.
- Harris, I., Jones, P.D., Osborn, T.J., Lister, D.H., 2014. Updated high-resolution grids of monthly climatic observations—the CRU TS. 10 dataset. *Int. J. Climatol.* 34 (3), 623–642. <https://doi.org/10.1002/joc.3711>.
- Hu, Y.F., Hu, Y., 2019. Land cover changes and their driving mechanisms in Central Asia from 2001 to 2017 supported by Google Earth Engine. *Remote Sens.* 11 (5), 1–21. <https://doi.org/10.3390/rs11050554>.

- Hua, T., Zhao, W.W., Liu, Y.X., Wang, S., Yang, S.Q., 2018. Spatial consistency assessments for global land-cover datasets: a comparison among GLC2000, CCI LC, MCD12, GLOBCOVER and GLCNMO. *Remote Sens.* 10 (1846), 1–18. <https://doi.org/10.3390/rs10111846>.
- Huang, W., Chen, F.H., Feng, S., Chen, J.H., Zhang, X.J., 2013. Interannual precipitation variations in the mid-latitude Asia and their association with large-scale atmospheric circulation. *Chin. Sci. Bull.* 58 (32), 3962–3968. <https://doi.org/10.1007/s11434-013-5970-4>.
- Huang, J.P., Li, Y., Fu, C., Chen, F., Fu, Q., Dai, A., Shinoda, M., Ma, Z., Guo, W., Li, Z., Zhang, L., Liu, Y., Yu, H., He, Y., Xie, Y., Guan, X., Ji, M., Lin, L., Wang, S., Yan, H., Wang, G., 2017. Dryland climate change: recent progress and challenges. *Rev. Geophys.* 55 (3), 719–778. <https://doi.org/10.1002/2016RG000550>.
- Indoitu, R., Kozhordan, G., Batyrbaeva, M., Vitkovskaya, I., Orlovsky, N., Blumberg, D., Orlovsky, L., 2015. Dust emission and environmental changes in the dried bottom of the Aral Sea. *Aeolian Res.* 17, 101–115. <https://doi.org/10.1016/j.aeolia.2015.02.004>.
- Jiang, L.L., Jiaqaaer, G., Bao, A.M., Guo, H., Ndayisaba, F., 2017. Vegetation dynamics and responses to climate change and human activities in Central Asia. *Sci. Total Environ.* 599, 967–980. <https://doi.org/10.1016/j.scitotenv.2017.05.012>.
- Jin, Q.J., Wei, J.F., Yang, Z.L., Lin, P.R., 2017. Irrigation-induced environmental changes around the Aral Sea: an integrated view from multiple satellite observations. *Remote Sens.* 9 (900), 1–13. <https://doi.org/10.3390/rs9090900>.
- Kendall, M., 1975. *Rank Correlation Methods*. Charles Griffin, London (Google Scholar).
- Khan, V.M., Holko, L., 2009. Snow cover characteristics in the Aral Sea basin from different data sources and their relation with river runoff. *J. Mar. Syst.* 76 (3), 254–262. <https://doi.org/10.1016/j.jmarsys.2008.03.012>.
- Khan, M.S., Liaqat, U.W., Baik, J.J., Choi, M.H., 2018. Stand-alone uncertainty characterization of GLEAM, GLDAS and MOD16 evapotranspiration products using an extended triple collocation approach. *Agric. For. Meteorol.* 252, 256–268. <https://doi.org/10.1016/j.agrformet.2018.01.022>.
- Kienzler, K.M., Lamers, J.P.A., McDonald, A., Ibragimov, N., Egamberdiev, O., Ruzibaev, E., Akramkhanov, A., 2012. Conservation agriculture in Central Asia—what do we know and where do we go from here? *Field Crop Res.* 132, 95–105. <https://doi.org/10.1016/j.fcr.2011.12.008>.
- Klein, I., Gessner, U., Kuenzer, C., 2012. Regional land cover mapping and change detection in Central Asia using MODIS time-series. *Appl. Geogr.* 35 (1–2), 219–234. <https://doi.org/10.1016/j.apgeog.2012.06.016>.
- Kozhordan, G., Orlovsky, L., Orlovsky, N., 2012. Monitoring land cover dynamics in the Aral Sea region by remote sensing. *Earth Resources and Environmental Remote Sensing/GIS Applications III*. 85381v. International Society for Optics and Photonics, pp. 1–9. <https://doi.org/10.1117/12.972306>.
- Li, Z., Chen, Y.N., Li, W.H., Deng, H.J., Fang, G.H., 2015. Potential impacts of climate change on vegetation dynamics in Central Asia. *J. Geophys. Res. Atmos.* 120 (24), 12345–12356. <https://doi.org/10.1002/2015JD023618>.
- Li, Q., Nian, Y.Y., Li, X., 2017. *The analysis of spatial and temporal change in the Amu Darya basin, Central Asia, from 2000 to 2009*. *Remote Sens. Technol. Appl.* 32 (2), 218–227.
- Li, W., MacBean, N., Ciais, P., Defourny, P., Lamarche, C., Bontemps, S., Houghton, R.A., Peng, S.S., 2018a. Gross and net land cover changes in the main plant functional types derived from the annual ESA CCI land cover maps. *Earth Syst. Sci. Data* 10 (1), 119–234. <https://doi.org/10.5194/essd-10-219-2018>.
- Li, X., Cheng, G.D., Ge, Y.C., Li, H., Han, F., Hu, X., Cai, X., 2018b. Hydrological cycle in the Heihe River basin and its implication for water resource management in endorheic basins. *J. Geophys. Res. Atmos.* 123 (2), 890–914. <https://doi.org/10.1002/2017JD027889>.
- Li, J.Y., Chen, H.X., Zhang, C., Pan, T., 2019. Variations in ecosystem service value in response to land use/land cover changes in Central Asia from 1995–2035. *PeerJ* 7, e7665. <https://doi.org/10.7717/peerj.7665>.
- Li, Q., Li, X., Ran, Y.H., Feng, M., Nian, Y.Y., Tan, M.B., Chen, X., 2021. Investigate the relationships between the Aral Sea shrinkage and the expansion of cropland and reservoir in its drainage basins between 2000 and 2020. *Int. J. Digit. Earth* <https://doi.org/10.1080/17538947.2020.1865466>.
- Liang, L., Liu, Q.S., Liu, G.H., Li, H., Huang, C., 2019. Accuracy evaluation and consistency analysis of four global land cover products in the arctic region. *Remote Sens.* 11 (1396), 1–24. <https://doi.org/10.3390/rs11121396>.
- Lioubimtseva, E., 2014. Impact of climate change on the Aral Sea and its basin. *The Aral Sea*. Springer, Berlin, Heidelberg, pp. 405–427. https://doi.org/10.1007/978-3-642-02356-9_17 Chapter17.
- Lioubimtseva, E., 2015. A multi-scale assessment of human vulnerability to climate change in the Aral Sea basin. *Environ. Earth Sci.* 73 (2), 719–729. <https://doi.org/10.1007/s12665-014-3104-1>.
- Liu, Q.H., Zhang, Y.L., Liu, L.S., Li, L.H., Qi, W., 2019. The spatial local accuracy of land cover datasets over the Qiangtang Plateau, High Asia. *J. Geogr. Sci.* 29 (11), 1841–1858. <https://doi.org/10.1007/s11442-019-1992-0>.
- Liu, S., Luo, G.P., Wang, H., 2020. Temporal and spatial changes in crop water use efficiency in Central Asia from 1960 to 2016. *Sustainability* 12 (572), 1–18. <https://doi.org/10.3390/su12020572>.
- López, P.L., Sutanudjaja, E.H., Schellekens, J., Sterk, G., Bierkens, M.F.P., 2017. Calibration of a large-scale hydrological model using satellite-based soil moisture and evapotranspiration products. *Hydrol. Earth Syst. Sci.* 21 (6), 3125–3144. <https://doi.org/10.5194/hess-21-3125-2017>.
- Löw, F., Navratil, P., Kotte, K., Schöler, H.F., Bubenzier, O., 2013. Remote-sensing-based analysis of landscape change in the desiccated seabed of the Aral Sea—a potential tool for assessing the hazard degree of dust and salt storms. *Environ. Monit. Assess.* 185 (10), 8303–8319. <https://doi.org/10.1007/s10661-013-3174-7>.
- Löw, F., Prishchepov, A.V., Waldner, F., Dubovik, O., Akramkhanov, A., Biradar, C., Lamers, J.P.A., 2018. Mapping cropland abandonment in the Aral Sea basin with MODIS time series. *Remote Sens.* 10 (159), 2–24. <https://doi.org/10.3390/rs10020159>.
- Luan, W.F., Li, X., 2021. Rapid urbanization and its driving mechanism in the Pan-Third pole region. *Sci. Total Environ.* 750, 141270. <https://doi.org/10.1016/j.scitotenv.2020.141270>.
- Mann, H.B., 1945. Nonparametric tests against trend. *Econometrica J. Econ. Soc.*, 245–259. <https://doi.org/10.2307/1907187>.
- Martens, B., Miralles, D.G., Lievens, H., Van Der Schalie, R., De Jeu, R.A.M., Fernández-Prieto, D., Beck, H.E., Dorigo, W.A., Verhoest, N.E.C., 2017. GLEAM v3: satellite-based land evaporation and root-zone soil moisture. *Geosci. Model Dev.* 10 (5), 1903–1925. <https://doi.org/10.5194/gmd-10-1903-2017>.
- Massakbayeva, A., Abuduwaili, J., Bissenbayeva, S., Issina, B., Smanov, Z., 2020. Water balance of the Small Aral Sea. *Environ. Earth Sci.* 79 (75), 1–11. <https://doi.org/10.1007/s12665-019-8739-5>.
- Micklin, P., 1992. The Aral crisis: introduction to the special issue. *Post-Soviet Geogr.* 33 (5), 269–282. <https://doi.org/10.1080/10605851.1992.10640900>.
- Micklin, P., 2004. *The Aral Sea Crisis, Dying and Dead Seas Climatic Versus Anthropic Causes*. Springer, pp. 99–123.
- Micklin, P., 2010. The past, present, and future Aral Sea. *Lakes Reserv. Res. Manag.* 15 (3), 193–213. <https://doi.org/10.1111/j.1440-1770.2010.00437.x>.
- Micklin, P., 2016. The future Aral Sea: hope and despair. *Environ. Earth Sci.* 75 (9), 1–15. <https://doi.org/10.1007/s12665-016-5614-5>.
- Micklin, P., Aladin, N.V., 2008. Reclaiming the Aral Sea. *Sci. Am.* 298 (4), 64–71. <https://www.jstor.org/stable/26000560>.
- Micklin, P., Aladin, N.V., Plotnikov, I., 2014. *The Aral Sea: The Devastation and Partial Rehabilitation of a Great Lake*. Springer.
- Mitchell, T.D., Jones, P.D., 2005. An improved method of constructing a database of monthly climate observations and associated high-resolution grids. *Int. J. Climatol.* 25 (6), 693–712. <https://doi.org/10.1002/joc.1181>.
- Pijanowski, B.C., Brown, D.G., Shellito, B.A., Manik, G.A., 2002. Using neural networks and GIS to forecast land use changes: a land transformation model. *Comput. Environ. Urban Syst.* 26 (6), 553–575. [https://doi.org/10.1016/S0198-9715\(01\)00015-1](https://doi.org/10.1016/S0198-9715(01)00015-1).
- Ruan, H.W., Yu, J.J., Wang, P., Wang, T.Y., 2020. Increased crop water requirements have exacerbated water stress in the arid transboundary rivers of Central Asia. *Sci. Total Environ.* 713 (136585), 1–11. <https://doi.org/10.1016/j.scitotenv.2020.136585>.
- Saiko, T.A., Zonn, I.S., 2000. Irrigation expansion and dynamics of desertification in the Circum-Aral region of Central Asia. *Appl. Geogr.* 20 (4), 349–367. [https://doi.org/10.1016/S0143-6228\(00\)00014-X](https://doi.org/10.1016/S0143-6228(00)00014-X).
- Sang, L.L., Zhang, C., Yang, J.Y., Zhu, D.H., Yun, W.J., 2011. Simulation of land use spatial pattern of towns and villages based on CA-Markov model. *Math. Comput. Model.* 54 (3–4), 938–943. <https://doi.org/10.1016/j.mcm.2010.11.019>.
- Shen, H., Abuduwaili, J., Ma, L., Samat, A., 2019. Remote sensing-based land surface change identification and prediction in the Aral Sea bed, Central Asia. *Int. J. Environ. Sci. Technol.* 16 (4), 2031–2046. <https://doi.org/10.1007/s13762-018-1801-0>.
- Shi, W., Wang, M.H., Guo, W., 2014. Long-term hydrological changes of the Aral Sea observed by satellites. *J. Geophys. Res. Oceans* 119 (6), 3313–3326. <https://doi.org/10.1002/2014JC009988>.
- Shibuo, Y., Jarsjö, J., Destouni, G., 2007. Hydrological responses to climate change and irrigation in the Aral Sea drainage basin. *Geophys. Res. Lett.* 34 (L21406), 1–5. <https://doi.org/10.1029/2007GL031465>.
- Singh, A., Seitz, F., Schwatke, C., 2012. Inter-annual water storage changes in the Aral Sea from multi-mission satellite altimetry, optical remote sensing, and GRACE satellite gravimetry. *Remote Sens. Environ.* 123, 187–195. <https://doi.org/10.1016/j.rse.2012.01.001>.
- Small, E.E., Giorgi, F., Sloan, L.C., Hostetler, S., 2001. The effects of desiccation and climatic change on the hydrology of the Aral Sea. *J. Clim.* 14 (3), 300–322. [https://doi.org/10.1175/1520-0442\(2001\)013%3C0300:TEODAC%3E2.0.CO;2](https://doi.org/10.1175/1520-0442(2001)013%3C0300:TEODAC%3E2.0.CO;2).
- Spoor, M., 1998. The Aral Sea basin crisis: transition and environment in former soviet Central Asia. *Dev. Chang.* 29 (3), 409–435. <https://doi.org/10.1111/1467-7660.00084>.
- Strikeleva, E., Abdullaev, I., Reznikova, T., 2018. Influence of land and water rights on land degradation in Central Asia. *Water* 10 (1242), 1–11. <https://doi.org/10.3390/w10091242>.
- Tsendbazar, N.E., De Bruin, S., Herold, M., 2015. Assessing global land cover reference datasets for different user communities. *ISPRS J. Photogram. Remote Sens.* 103, 93–114. <https://doi.org/10.1016/j.isprsjprs.2014.02.008>.
- Wang, X.L., Luo, Y., Sun, L., He, C.S., Zhang, Y.Q., Liu, S.Y., 2016. Attribution of runoff decline in the Amu Darya River in Central Asia during 1951–2007. *J. Hydrometeorol.* 17 (5), 1543–1560. <https://doi.org/10.1175/JHM-D-15-0114.1>.
- Wang, L.B., Bartlett, P., Pouliot, D., Chan, E., Lamarche, C., Wulder, M.A., Defourny, P., Brady, M., 2019a. Comparison and assessment of regional and global land cover datasets for use in class over Canada. *Remote Sens.* 11 (2286), 1–25. <https://doi.org/10.3390/rs11192286>.
- Wang, X.F., Xiao, J.F., Li, X., Cheng, G.D., Ma, M.G., Zhu, G.F., Arain, M.A., Black, T.A., Jassal, R.S., 2019b. No trends in spring and autumn phenology during the global warming hiatus. *Nat. Commun.* 10 (1), 1–10. <https://doi.org/10.1038/s41467-019-10235-8>.
- Wang, X.X., Chen, Y.N., Li, Z., Fang, G.H., Wang, F., Liu, H.J., 2020. The impact of climate change and human activities on the Aral Sea basin over the past 50 years. *Atmos. Res.* 245. <https://doi.org/10.1016/j.atmosres.2020.105125>.
- Wei, W., Zhu, Y.J., Li, H., Zhang, K.B., Wang, B.T., Yang, X.H., Shi, Z.J., 2018. Spatio-temporal reorganization of cropland development in Central Asia during the post-soviet era: a sustainable implication in Kazakhstan. *Sustainability* 10 (4042), 1–20. <https://doi.org/10.3390/su10114042>.

- Welford, B.P., 1970. Mathematical model building in economics and industry. *J. R. Stat. Soc.: Ser. C: Appl. Stat.* 19 (1), 102.
- Wurtsbaugh, W.A., Miller, C., Null, S.E., DeRose, R.J., Wilcock, P., Hahnberger, M., Howe, F., Moore, J., 2017. Decline of the world's saline lakes. *Nat. Geosci.* 10 (11), 816–821. <https://doi.org/10.1038/ngeo3052>.
- Xu, H.J., Wang, X.P., Zhang, X.X., 2016. Decreased vegetation growth in response to summer drought in Central Asia from 2000 to 2012. *Int. J. Appl. Earth Observ. Geoinform.* 52, 390–402. <https://doi.org/10.1016/j.jag.2016.07.010>.
- Yang, Y.K., Xiao, P.F., Feng, X.Z., Li, H.X., 2017. Accuracy assessment of seven global land cover datasets over China. *ISPRS J. Photogramm. Remote Sens.* 125, 156–173. <https://doi.org/10.1016/j.isprsjprs.2017.01.016>.
- Zhang, J.Y., Chen, Y.N., Li, Z., 2018. Assessment of efficiency and potentiality of agricultural resources in Central Asia. *J. Geogr. Sci.* 28 (9), 1329–1340. <https://doi.org/10.1007/s11442-018-1528-3>.
- Zhang, J.Y., Chen, Y.N., Li, Z., Song, J.X., Fang, G.H., Li, Y.P., Zhang, Q.F., 2019. Study on the utilization efficiency of land and water resources in the Aral Sea basin, Central Asia. *Sustain. Cities Soc.* 51 (101693), 1–9. <https://doi.org/10.1016/j.scs.2019.101693>.
- Zhou, Y., Zhang, L., Fensholt, R., Wang, K., Vitkovskaya, I., Tian, F., 2015. Climate contributions to vegetation variations in Central Asian drylands: pre-and post-USSR collapse. *Remote Sens.* 7 (3), 2449–2470. <https://doi.org/10.3390/rs70302449>.
- Zhou, Y., Zhang, L., Xiao, J.F., Williams, C.A., Vitkovskaya, I., Bao, A.M., 2019. Spatiotemporal transition of institutional and socioeconomic impacts on vegetation productivity in Central Asia over last three decades. *Sci. Total Environ.* 658, 922–935. <https://doi.org/10.1016/j.scitotenv.2018.12.155>.
- Zou, S., Jilili, A., Duan, W., Maeyer, P.D., de Voorde, T.V., 2019. Human and natural impacts on the water resources in the Syr Darya River basin, Central Asia. *Sustainability* 3084 (11), 1–18. <https://doi.org/10.3390/su1113084>.